Biosystems Engineering

Estimation models for the aerodynamic characterisation of insect-proof screens from their geometric parameters

--Manuscript Draft--

Manuscript Number:	YBENG-D-19-00039R2
Article Type:	Research Paper
Keywords:	insect-proof screen; aerodynamic characterisation; aerodynamic model.
Corresponding Author:	Alejandro López Martínez Universidad de Almería Almería, Almeria Spain
First Author:	Alejandro López-Martínez
Order of Authors:	Alejandro López-Martínez
	Francisco Domingo Molina-Aiz, Professor
	Diego Luis Valera-Martínez, Professor
	Karlos Emmanuel Espinoza-Ramos
Manuscript Region of Origin:	Europe
Abstract:	This study characterised the geometric and aerodynamic parameters of 35 insect-proof screens with different weft and warp threads, with porosities ranging from 0.237 to 0.556 m2 m-2. The geometric parameters were assessed by analysing digital images, and the aerodynamic parameters were determined using tests in a low-speed wind tunnel. Using the experimental measurements, four different models were developed and validated to estimate the aerodynamic parameters of an insect-proof screen from two or more of their geometric parameters: (i) to estimate the pressure drop coefficient Fφ based on the thread diameter Reynolds number (Red) and screen porosity φ [m2 m-2] Fφ=(0.4810002+11.5331/Red)×((1–φ2)/φ2) (R2 = 93.9% with a p-value = 0.000); (ii) estimating Fφ based on the screen thickness Reynolds number (Ret) and screen porosity φ [m2 m-2] Fφ = (0.475502+26.2114/Ret)×((1–φ2)/φ2) (R2 = 92.1% with a p-value = 0.000); (iii) estimating screen permeability Kp=Dh2φ3/(2.0679 (1–φ)2)+3.8362×10–10 (R2=56.3%//56.2 % with a p-value<0.05) as a function of thread diameter Dh [m] and porosity φ [m2 m-2]; (iv) estimating the inertial factor Y=0.0571195+0.135966· Dh/Di (R2=58.1% with a p-value=0.0000) as a function of thread diameter [m] and the inner pore diameter Di [m]. These models gave improved accuracy compared with the previous models described in the literature. Models for aerodynamic parameters of the insect-proof screens Kp and Y based in their geometric characteristics are very important to simulate the effects of insect screens in ventilation studies using computational fluid dynamic (CFD) studies.
Opposed Reviewers:	
Response to Reviewers:	Thank you, we have reviewed the document. We have accepted all changes. We have also made the improvements suggested by the editor. We have marked in color the changes made.

Editor comments:

Thank you for making the changes required by the reviewers. Your paper is basically acceptable for publication but requires minor changes.

I have carried out a technical edit on your submission using Word Track Changes and suggested changes. You may access my edited version in the attachment. Please check my edits carefully as I may not have always understood your original meaning.

Please also check my comments.

I also suggest that you carefully examine the journal Guide for Authors available through the journal web site.

I look forward to shortly receiving a revised manuscript and moving to accept it for publication.

Thank you, we have reviewed the document. We have accepted all changes. We have also made the improvements suggested by the editor.

We have marked in color the changes made.

Highlights

Different models estimated aerodynamic characteristics from geometric parameters

Pressure drop coefficient estimated from screen porosity using Re based on thread diameter

Pressure drop coefficient also estimated from porosity and Re based on thread thickness

Permeability estimated from pore surface area or thread diameter & screen porosity

Inertial factor estimated from screen porosity or thread diameter & inner pore diameter

Models for characterising the aerodynamics of insect-proof screens from their geometric parameters

A. López-Martínez[1,*], F.D. Molina-Aiz[1], D.L. Valera-Martínez[1] and K.E. Espinoza-Ramos[2]

[1]CIAIMBITAL Research Centre, University of Almería, Ctra. de Sacramento s/n, 04120 Almería, Spain; alexlopez@ual.es (A.L.-M.); fmolina@ual.es (F.D.M.-A.); dvalera@ual.es (D.L.V.-M.);

[2]Department of Engineerings, University Center of the South Coast, University of Guadalajara. Av. Independencia Nacional 151, Autlán de Navarro, Jalisco 48900, México; karlos.espinoza@cucsur.udg.mx (K.E.E.-R);

[*]Corresponding author: alexlopez@ual.es; Tel.: +34-950-21-4231

Abstract

This study characterised the geometric and aerodynamic parameters of 35 insect-proof screens with different weft and warp threads, with porosities ranging from 0.237 to 0.556 m^2 m^{-2}. The geometric parameters were assessed by analysing digital images, and the aerodynamic parameters were determined using tests in a low-speed wind tunnel. Using the experimental measurements, four different models were developed and validated to estimate the aerodynamic parameters of an insect-proof screen from two or more of their geometric parameters: (i) to estimate the pressure drop coefficient F_φ based on the thread diameter Reynolds number (Re_d) and screen porosity φ [m^2 m^{-2}] $F_\varphi=(0.4810002+11.5331/Re_d)\times((1-\varphi^2)/\varphi^2)$ (R^2 = 93.9% with a *p*-value = 0.000); (ii) estimating F_φ based on the screen thickness Reynolds number (Re_t) and screen porosity φ [m^2 m^{-2}] $F_\varphi = (0.475502+26.2114/Re_t)\times((1-\varphi^2)/\varphi^2)$ (R^2 = 92.1% with a *p*-value = 0.000); (iii) estimating screen permeability $K_p=D_h^2\varphi^3/(2.0679\ (1-\varphi)^2)+3.8362\times10^{-10}$ (R^2=56.3%//56.2 % with a *p*-value<0.05) as a function of thread diameter D_h [m] and porosity φ [m^2 m^{-2}]; (iv) estimating the inertial factor $Y=0.0571195+0.135966\cdot D_h/D_i$ (R^2=58.1% with a *p*-value=0.0000) as a function of thread diameter [m] and the inner pore diameter D_i [m]. These

models gave improved accuracy compared with the previous models described in the literature. Models for aerodynamic parameters of the insect-proof screens K_p and Y based in their geometric characteristics are very important to simulate the effects of insect screens in ventilation studies using computational fluid dynamic (CFD) studies.

Keywords: insect-proof screen; aerodynamic characterisation; aerodynamic model.

Nomenclature

Abbreviations:

MD	Bias
NSE	Nash-Sutcliffe efficiency
PBIAS	Percent bias
RMSD	Root mean squared deviation
RSR	*RMSD*-observations standard deviation ratio

Symbols:

a and b	Second-order polynomial regression coefficients
e	Thickness [µm]
n	Number of values
u	Air speed [m s^{-1}]
x	Direction of airflow
A and B	Constants that depend on the type of porous material
C_d	Total discharge coefficient of a greenhouse opening
$C_{d,\varphi}$	Discharge coefficient due to the presence of insect-proof screens
D_f	Thread density according to the manufacturer [threads cm^{-2}]
D_h	Diameter of the threads [µm]
D_{hx}	Diameter of the weft threads [µm]
D_{hy}	Diameter of the warp threads [µm]

D_i	Diameter of the inside circumference of the pore [μm]
D_r	Thread density measurement [threads cm^{-2}]
F_φ	Pressure drop coefficient due to the presence of an insect-proof screen
K_p	Screen permeability [m^2]
L_{px}	Length of the pore in the direction of the weft [μm]
L_{py}	Length of the pore in the direction of the warp [μm]
P	Pressure [Pa]
R	Coefficient of correlation
R^2	Coefficient of determination
Re_p	Reynolds number based on the thread screen's permeability
Re_d	Reynolds number based on the diameter of the threads of the screen
Re_t	Reynolds number based on the thickness of the screen.
S_p	Area of the pore [mm^2]
Y	Inertial factor

Greek Symbols:

μ	Dynamic viscosity of air [kg s^{-1} m^{-1}]
φ	Porosity [m^2 m^{-2}]
β	Constant that depend on the type of porous material
ρ_a	Density of air [kg m^{-3}]
Δ	Difference

Subscripts:

obs	Values observed experimentally with wind tunnel tests
sim	Values simulated or obtained with models

1. *Introduction*

Insect-proof screens, placed in greenhouse vents, are used throughout the world to protect crops against insects pests. In many regions, such as the Mediterranean, screens are normally fitted to all vents in intensive greenhouse production. A recently published study showed that 99.1% of farmers in the province of Almería (Spain) install insect-proof screens in all side vents, and 95.4% of farmers install them in the roof vents of their greenhouses (Valera *et al*., 2016). The survey showed that 58.3% of the screens installed in the vents had a thread density of 15×30 threads cm^{-2} and 25.6% had a density of 10×20 threads cm^{-2}; the percentages for roof vents were 56.0% and 22.5%, respectively (Valera *et al*., 2016). The use of these screens reduces the number of insect that enter the greenhouse, thereby decreasing the need for crop protection chemical treatments (Berlinger *et al*., 1993; Taylor *et al*., 2001; Teitel, 2007) and preventing beneficial insects, such as pollinating insects (Teitel, 2007) or those used in integrated insect pest management, from leaving the greenhouse.

Numerous studies show the disadvantages of installing these screens, which adversely affect the ventilation rate of a greenhouse (defined as the number of times that the greenhouse air is renewed in one hour, h^{-1}) and, therefore, its microclimate (Muñoz *et al*., 1999; Miguel and Silva, 2000; Bartzanas *et al*., 2002; Fatnassi *et al*., 2002, 2003 and 2006; Soni *et al*., 2005; Harmanto *et al*., 2006; Kittas *et al*., 2008; Teitel, 2007 and 2010; López *et al*., 2014). Compared with greenhouses without insect-proof screens, greenhouses with screens have higher temperature and humidity (Bartzanas *et al*., 2002; Fatnassi *et al*., 2002, 2003 and 2006; Harmanto *et al*., 2006), lower air velocity (Kittas *et al*., 2008) and a greater vertical temperature gradient (Soni *et al*., 2005); all these characteristics can adversely affect crop growth and development (Kittas *et al*., 2002; Teitel, 2010).

Insect-proof screens affect greenhouse ventilation flow and produces an additional pressure drop to that produced by the geometry of the windows (characterised by a vent discharge coefficient C_d). This pressured drop can be related to the velocity of air crossing the openings

(u) (Teitel, 2007; Molina-Aiz *et al*., 2009) using only a quadratic term (ΔP = a u^2) or a quadratic polynomial (ΔP = a u^2 + b u). In the first case, the aerodynamic behaviour of the screens is characterised using only one parameter, a pressure drop coefficient (F_φ) but in the second case, two parameters are required, permeability (K_p), that is independent of the nature of the fluid but depends on the geometry of the porous medium, and an inertial factor (Y) that varies with the nature of the porous medium but can be as small as 0.1 in the case of foam metal fibres (Nield and Bejan, 1999). Thus, knowing the aerodynamic characteristics of insect-proof screens (F_φ or K_p and Y) enables the effects of their use in a greenhouse with a known ventilation rate to be estimated.

Accurate determination of the aerodynamic characteristics of insect-proof screens requires either wind tunnel tests and assessment of the geometric characteristics of screens. Models have been developed for estimating the pressure drop coefficient of a screen (F_φ) from its Reynolds number based on the thread diameter (Re_d) and from its porosity (φ) (Hayama *et al*., 2000; Pinker and Herbert, 1967; Linker *et al*., 2002; Bailey *et al*., 2003). Both thread diameter (D_h) and porosity (φ), can be determined by processing digital images of insect-proof screens (Álvarez *et al*., 2012). Porosity can be estimated using most image processing software to count black and white pixels, or it can be estimated using specific software such as Euclides v1.4, proposed by Álvarez *et al*. (2012). This specialist software determines screen porosity by identifying the coordinates of the vertices of the screen pores, thus providing a value of screen porosity while maintaining an adequate ratio between the areas of the image occupied by pores and threads. The thread diameter of the screen can also be assessed through direct measurements with a micrometer, but manually determining thread diameter can be a very laborious task.

The objective of this study was to develop different models for estimating the pressure drop caused by an insect-proof screen at a specific air velocity from its geometric characteristics.

Thus, depending on the ability to estimate geometric or other parameters, a specific model may be selected to estimate the aerodynamic characteristics of an insect-proof screen. The first model investigated estimated F_φ as a function of porosity (φ) and Reynolds number (Re_t) based on screen thickness (e); the second model estimated F_φ as a function of porosity (φ) and Reynolds number Re_d based on screen thread diameter (D_h). After estimating F_φ, a graph of pressure drop as a function of air velocity can be developed. A third model was proposed for estimating screen permeability (K_p) as a function of thread diameter (D_h) and porosity (φ). A further model was proposed for estimating screen inertial factor (Y) as a function of thread diameter (D_h) and inner pore diameter (D_i). After estimating K_p and Y, and knowing the screen thickness (e), a screen pressure drop graph can be developed.

2. *Material and methods*

To develop different models for estimating the aerodynamic characteristics of an insect-proof screen from only its geometric characteristics, 35 insect-proof screens with different thread densities were analysed (Table 1). Insect-proof screens are manufactured with high-density polyethylene (HDPE) monofilament-woven fabrics, with knot-free weft and warp threads (Fig. 1). This type of insect-proof screen is used in all greenhouses in the province of Almería, Spain (Valera *et al*. 2016) and is the type most commonly used in greenhouses worldwide.

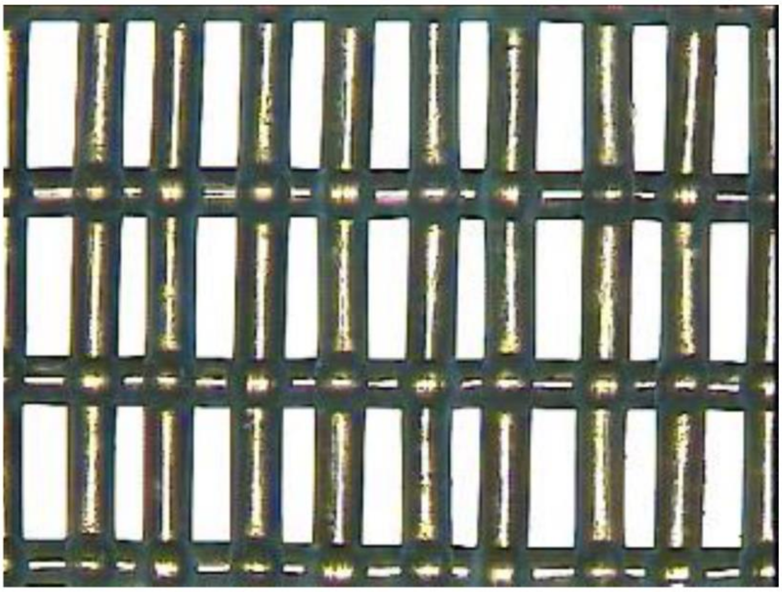

Fig. 1. Microscopic image (4×) of a 14×27 threads cm^{-2} insect-proof screen

2.1. ***Determining the geometric characteristics of insect-proof screens***

The two-dimensional geometric characteristics of insect-proof screens were assessed by processing digital images acquired with a Motic DMWB1-223 microscope (Motic Spain S.L., Barcelona) equipped with a digital camera, and with a 4× calibrated microscope lens (with a resolution of 10.5 μm pixel^{-1}). Three samples were analysed for each screen, acquiring 24 0.34 × 0.25 cm^2 images per sample. The method used to determine the geometric characteristics of insect-proof screens is available from López *et al*. (2013). The specific software Euclides v1.4 (Álvarez, 2010; Álvarez *et al*., 2012) was used to identify the vertices of each pore (Fig. 2a). From these vertices, the following two-dimensional geometric parameters were obtained (Table 1 and Fig. 2b): D_r, measured thread density [threads cm^{-2}]; φ, porosity [m^2 m^{-2}]; L_{px} and L_{py}, the lengths of the pore [μm] in the weft and warp directions, respectively; D_{hx} and D_{hy}, diameter [μm] of the weft and warp threads, respectively; D_h, diameter of the threads [μm]; D_i, inner pore diameter [μm]; S_p, pore area [mm^2]. For each image acquired, approximately 12 (for 10 × 20 threads cm^{-2} screens), 27 (for 14 × 27 threads cm^{-2} screens) and 30 (for 13 × 30 threads cm^{-2} screens) pores were analysed giving a total of 864, 1944 and 2160 pores analysed per screen, respectively. Álvarez *et al*. (2012) made an exhaustive analysis where they showed that three randomly selected samples were sufficient to geometrically characterise these types of screen.

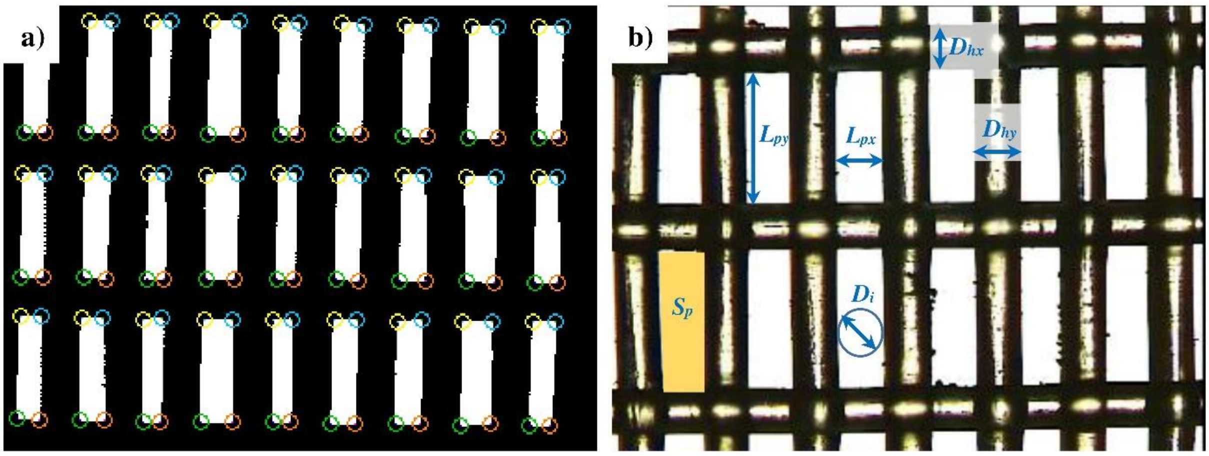

Fig. 2. Image of a 14 × 27 threads cm^{-2} insect-proof screen with identified pore vertices (a). Geometric parameters indicated on a 10 × 20 threads cm^{-2} screen (b).

The thickness (*e*) of the insect-proof screens has been measured with a TESA-VISIO 300 device (TESA SA, Switzerland; resolution of 0.05 µm) through non-contact optical measurement. For the magnitude of the measurements *e*, the uncertainty was <10 µm.

Table 1. Geometric characteristics of the insect-proof screens (D_f, thread density according to the manufacturer [threads cm^{-2}]). Average value and standard deviation of: D_r, measured thread density [threads cm^{-2}]; φ, porosity [m^2 m^{-2}]; L_{px} and L_{py}, the lengths of the pore [µm] in the weft and warp directions, respectively; D_{hx} and D_{hy}, diameter [µm] of the weft and warp threads, respectively; D_h, diameter of the threads [µm]; D_i, diameter of the inside circumference of the pore [µm]; S_p, area of the pore [mm^2]; e, thickness [m].

N	D_f	D_r	φ	L_{px}	L_{py}	D_{hx}	D_{hy}	D_h	D_i	S_p	e [×10^{-6}]
1	11×23	10.4×22.2	0.322±0.008	197.0±15.1	709.5±30.5	248.2±8.4	254.4±10.6	251.3±10.3	202.0±15.1	0.140±0.012	589±7
2*	10×20	9.8×20.1	0.369±0.012	243.7±25.1	774.0±61.0	251.6±7.7	253.5±8.3	252.5±8.1	248.5±25.0	0.189±0.025	596±8
3	10×20	10.1×20.6	0.366±0.006	232.5±18.8	760.7±25.7	233.1±6.2	253.1±9.0	243.1±12.6	237.4±18.6	0.177±0.015	544±7
4	10×20	10.7×21.3	0.349±0.009	226.9±20.1	681.1±26.5	256.8±6.0	243.5±11.3	250.2±11.6	232.1±20.3	0.154±0.015	567±5
5	10×20	9.7×20.4	0.402±0.008	252.9±23.4	806.9±28.2	223.4±7.4	238.5±9.0	230.9±11.1	257.5±23.2	0.204±0.020	501±7
6	10×20	10.3×21.5	0.310±0.008	199.2±15.6	710.8±30.7	264.4±9.4	267.1±11.7	265.7±11.0	203.7±15.7	0.141±0.013	571±19
7	10×20	10.4×21.0	0.302±0.010	199.9±28.8	693.6±20.7	267.3±7.1	276.5±15.0	271.9±13.4	204.3±28.9	0.139±0.020	536±6
8	10×20	9.0×20.7	0.402±0.010	246.8±16.4	877.3±16.6	233.8±6.3	236.5±9.2	235.1±8.4	249.8±16.6	0.216±0.015	546±4
9	14×27	13.7×26.9	0.379±0.014	187.3±34.8	543.5±26.1	186.5±7.0	184.0±8.4	185.2±7.9	192.5±34.6	0.102±0.020	418±8
10	10×20	9.7×19.7	0.378±0.009	253.9±17.9	784.3±54.2	250.5±7.9	253.5±8.2	252.0±8.2	255.8±17.9	0.199±0.020	587±7
11	10×20	8.9×19.5	0.375±0.007	251.7±23.9	863.6±25.0	264.4±7.1	260.7±11.5	262.5±10.2	256.0±24.1	0.217±0.022	604±9
12	10×20	8.9×19.6	0.375±0.007	250.3±23.9	865.1±27.1	264.6±7.7	260.3±11.7	262.4±10.6	255.8±24.9	0.216±0.022	611±18
13	10×20	9.9×19.7	0.368±0.007	252.7±21.2	746.4±34.9	259.0±7.0	255.7±9.4	257.3±8.7	255.2±21.0	0.189±0.018	639±7
14	14×27	12.0×27.5	0.292±0.009	141.8±28.9	615.9±15.9	214.8±7.2	221.7±8.5	218.3±8.7	144.2±28.8	0.087±0.018	514±5
15	14×27	12.8×27.9	0.267±0.007	131.8±26.5	570.5±15.2	209.6±6.9	225.7±8.2	217.7±11.1	134.1±26.7	0.075±0.015	490±10
16	10×20	9.9×21.8	0.338±0.017	207.4±24.1	756.6±28.3	253.4±10.0	251.8±12.4	252.6±11.6	210.7±24.5	0.156±0.016	540±10
17	15×30	15.2×30.2	0.556±0.030	221.6±19.6	548.8±8.7	110.5±4.2	109.9±5.1	110.1±4.8	222.9±19.5	0.121±0.011	261±6
18	18×31	18.6×31.3	0.520±0.023	209.0±12.0	427.7±7.7	110.6±4.3	110.2±4.3	110.4±4.3	210.3±11.9	0.089±0.006	259±14
19	16×30	16.1×30.8	0.368±0.026	162.2±10.6	458.4±17.8	163.1±5.3	162.8±6.3	162.9±5.9	164.0±10.7	0.070±0.006	362±4
20	14×30	14.3×30.7	0.385±0.026	162.6±10.8	540.6±17.5	159.8±5.7	163.5±6.5	161.9±6.4	165.0±10.8	0.088±0.007	371±6
21	12×30	12.1×30.4	0.405±0.027	166.7±11.7	663.6±25.0	164.7±5.8	162.9±5.8	163.6±5.8	169.6±12.0	0.111±0.0009	388±6
22	10×30	9.6×30.2	0.437±0.029	170.9±13.8	876.8±27.9	163.3±5.3	160.0±5.9	161.2±5.9	174.5±14.2	0.150±0.013	406±6
23	10×30	9.4×30.2	0.446±0.043	173.0±20.0	900.9±125.4	158.1±5.6	158.4±5.4	158.3±5.5	177.2±20.0	0.156±0.029	419±27
24	13×30	13.1×30.5	0.390±0.006	164.6±9.3	593.3±19.0	168.6±6..6	163.1±6.3	165.5±7.0	167.4±9.6	0.098±0.006	392±5
25	10×20	9.9×19.7	0.335±0.011	233.7±23.9	734.0±29.2	276.4±11.2	273.4±10.7	274.5±11.0	236.6±24.0	0.171±0.019	564±6
26	14×27	12.9×26.8	0.385±0.006	188.4±25.7	591.6±28.2	184.1±7.2	184.7±7.1	184.4±7.1	191.3±25.6	0.111±0.016	402±15
27	10×20	9.2×20.7	0.375±0.007	234.9±16.1	838.7±27.0	245.8±7.1	248.0±8.3	247.2±7.9	238.7±16.4	0.197±0.015	526±26
28	10×20	10.1×20.0	0.379±0.007	256.6±14.3	736.4±17.1	256.8±8.3	243.7±8.2	248.6±10.4	259.8±14.4	0.189±0.011	480±11
29	13×30	12.5×31.3	0.263±0.005	110.0±7.9	611.9±17.5	187.7±6.7	209.4±8.2	200.2±13.1	113.5±8.5	0.067±0.005	458±44
30	10×20	9.8×20.0	0.350±0.008	238.6±19.5	746.0±22.7	272.0±7.2	261.2±12.4	265.3±11.9	241.7±19.5	0.178±0.015	564±45

31	15×30	15.3×31.4	0.237±0.006	107.5±14.6	456.3±20.8	196.0±7.6	211.1±7.6	204.7±10.7	110.7±16.7	0.049±0.008	508±33
32	10×20	9.6×20.3	0.360±0.007	239.9±18.5	765.4±27.1	272.2±11.6	252.0±8.6	259.6±13.9	241.9±19.1	0.182±0.015	508±19
33	10×20	9.2×19.9	0.381±0.008	250.6±17.7	829.1±37.1	257.5±8.5	251.3±8.6	253.6±9.1	255.0±17.7	0.208±0.017	504±12
34	10×20	9.7×19.9	0.381±0.014	254.1±22.3	777.7±25.3	253.6±6.9	247.2±11.1	249.6±10.2	257.2±22.6	0.198±0.018	535±7
35	10×20	9.8×19.9	0.354±0.007	240.0±18.0	761.5±23.7	264.0±7.8	261.8±9.3	262.6±8.8	242.8±17.8	0.183±0.015	535±10

* Screens 2 to 22 were analysed by Álvarez (2010).

2.2. *Determining the aerodynamic characteristics of insect-proof screens*

The aerodynamic characteristics of insect-proof screens were determined by tests using a wind tunnel (Fig. 3) designed at the University of Almería, Spain (Molina-Aiz *et al*., 2006; Valera *et al*., 2006), with an improved control system (Espinoza *et al*., 2015). The wind tunnel has a total length of 4.74 m and a 388 mm diameter test section, where the insect-proof screen samples were placed. Three tests were performed for each screen, with different, randomly selected samples (Espinoza *et al*., 2015; López *et al*., 2018). The wind tunnel had a maximum speed of 10 m s^{-1} and a maximum pressure drop of 200 Pa. These limits are set based on the air velocity characteristics and the wind tunnel pressure drop sensors. The pressure drop was recorded by two Pitot tubes (Airflow Developments Ltd, Buckinghamshire, UK; 4 mm of diameter) and with a differential pressure transducer SI727 (Special Instruments, Norlingen, Germany; operational range of 0-200 Pa and accuracy of ±0.25%). Air velocity and air temperature were measured by a hot-wire anemometer EE70-VT32C5 (Elektronik, Engerwitzdort, Austria; measurement range of 0-10 m s^{-1} and 0-50 ºC; accuracy of ±0.2 m s^{-1} + 2 % of measuring value and ±0.2 ºC). The technical characteristics of the wind tunnel and the control system used in this study are described in Espinoza *et al*. (2015). For each sample, a test sequence with nine increasing airspeeds or pressure drops was performed, followed by a sequence with nine decreasing airspeeds or pressure drops.

Fig. 3. Wind tunnel used for the tests

Curves of pressure drop ΔP [Pa] as a function of air velocity u [m s^{-1}] were constructed for each insect-proof screen. Insect-proof screens are porous media from which their aerodynamic parameters can be determined: K_p, the screen permeability [m^2], is a coefficient that depends on the geometry of the porous medium, and is independent of the nature of the fluid (Nield and Bejan, 1999); Y, the inertial factor [dimensionless], a drag constant that depends on the characteristics of the porous material; F_φ, the pressure drop coefficient.

Airflow through a porous medium can be described by modifying Darcy's equation (Forchheimer, 1901):

$$\frac{\partial P}{\partial x} = -\left(\frac{\mu}{K_p}\ u + \rho_a \left(\frac{Y}{K_p^{1/2}}\right) |u|\ u\right) \qquad (1)$$

where P is the pressure [Pa], x is the airflow direction, u is the air velocity [m s^{-1}], μ is the dynamic viscosity of air [kg s^{-1} m^{-1}] and ρ_a is the air density [kg m^{-3}]. To calculate both μ and ρ_a it was necessary to measure the air temperature (Molina-Aiz *et al*., 2004). Air temperature remained practically constant in each test (ranging from 19.8 and 25.5 ºC). Some authors have used a second-degree polynomial to fit the experimentally observed pressure drop values as a function of the airspeed passing through the porous medium (Miguel *et al*., 1997; Dierickx, 1998; Muñoz *et al*., 1999; Molina-Aiz *et al*., 2006; Valera *et al*., 2006). The zero-order term can be neglected (Miguel *et al*., 1997; Molina-Aiz *et al*., 2009; López *et al*., 2014), leading to the following equation:

$$\Delta P = au^2 + bu \quad (2)$$

By matching the first and second order coefficients of Eq. (2) with Eq. (1), the screen permeability (K_p) and its inertial factor (Y) can be determined as follows (Molina-Aiz *et al*., 2009):

$$K_p = e\,\frac{\mu}{b} \quad (3)$$

$$Y = \frac{a\,K_p^{0.5}}{\rho_a\,e} \quad (4)$$

Applying Eqs. (3) and (4) requires knowledge of the thickness (e) of the screens. Another way of describing the relationship between the pressure drop and airspeed is to use Bernoulli's equation (Kosmos *et al*., 1993; Montero *et al*., 1997; Teitel and Shklyar, 1998):

$$\Delta P = -{}^{1}\!/_{2}\,F_\varphi \rho_a u^2 \quad (5)$$

where F_φ is the pressure drop coefficient due to the presence of an insect-proof screen. The coefficient F_φ can be determined using Eqs. (1) and (5) since $\partial P/\partial x = \Delta P/e$ (Molina-Aiz *et al*., 2009):

$$F_\varphi = \frac{2\,e}{K_p^{0.5}}\left(\frac{1}{Re_p} + Y\right) \quad (6)$$

Below a specific Reynolds number limit, Teitel (2001) showed that the coefficient F_φ can be used to predict the pressure drop due to the screen. For a permeability-based Reynolds number (Re_p), the limit can be set to $Re_p < 10^5$ (Molina-Aiz *et al*., 2009). The permeability Reynolds number (Re_p) can be calculated by (Nield and Bejan, 1999):

$$Re_p = \frac{\sqrt{K_p}\,u\rho_a}{\mu} \quad (7)$$

Some authors have presented statistical models for predicting the value of F_φ as a function of porosity φ [m^2 m^{-2}] and Reynolds number (Re_d) based on the thread diameter (D_h) [m]: Eq. (8)

presented by Hayama *et al*. (2000) (in Bailey *et al*., 2003), Eq. (9) by Pinker and Herbert (1967) and Eq. (10) by Bailey *et al*. (2003):

$$F_\varphi = 28\left(\frac{Re_d\,\varphi^2}{1-\varphi}\right)^{-0.95} \tag{8}$$

$$F_\varphi = \left(\frac{13.0}{Re_d} + 0.82\right)\left(\frac{1-\varphi^2}{\varphi^2}\right) \tag{9}$$

$$F_\varphi = \left[\frac{18}{Re_d} + \frac{0.75}{log(Re_d+1.25)} + 0.055\,log(Re_d)\right]\left[\frac{1-\varphi^2}{\varphi^2}\right] \tag{10}$$

The Reynolds number Re_d is calculated from the air velocity [m s^{-1}] and the thread diameter (D_h) [m]:

$$Re_d = \frac{D_h u \rho_a}{\mu} \tag{11}$$

Another way of predicting the pressure drop in porous media is to use the equations presented in Nield and Bejan (1999) to estimate the K_p and Y values. The permeability (K_p) of the screen can be estimated from its porosity φ [m^2 m^{-2}] and fibre thread diameter D_h [m]. This expression is known as the Kozeny equation (Nield and Bejan, 1999):

$$K_p = \frac{{D_h}^2\varphi^3}{\beta(1-\varphi)^2} \tag{12}$$

where β is a constant that depends on the type of porous material. The inertial factor Y can be estimated from the fibre diameter and pore size (Beavers *et al*., 1973, Nield and Bejan, 1999), according to the following linear fit:

$$Y = A + B\frac{D_h}{D_i} \tag{13}$$

in which A and B are two constants that depend on the type of porous material. In the case of insect-proof screens, we should use the thread diameter D_h and the inner pore diameter D_i. Lastly, another method to estimate K_p and Y is to use the equations proposed by Miguel (1998) from the porosity φ [m^2 m^{-2}]:

$$K_p = 3.44 \times 10^{-9}\varphi^{1.6} \tag{14}$$

$$Y = 4.30 \times 10^{-2}\varphi^{-2.13} \tag{15}$$

After determining the aerodynamic characteristics of the 35 insect-proof screens in the wind tunnel, the goodness of fit of the proposed models was analysed by comparing the experimentally observed values of F_φ (tunnel tests) with the corresponding estimated values of F_φ according to Eqs. (8), (9) and (10), and proposing alternative models for estimating F_φ. The goodness of fit of the proposed models was also analysed by comparing the experimentally observed results (tunnel tests) and estimated values of K_p and Y according to Eqs. (12) and (13) and Eqs. (14-15), and similarly proposing alternative models for estimating K_p and Y.

2.3. *Statistical analysis*

Regression analyses were used to compare the different variables to obtain statistically significant relationships (p-value <0.05) using Statgraphics® Centurion 18 v18.1 (Statgraphics Technologies, Inc., The Plains, VA, USA). In addition to the correlation coefficient, R, other statistics were used to analyse the fit of the simulated (using different models) values of F_φ, K_p and Y to the experimentally observed values. Two of the most commonly used statistics for goodness of fit, based on the deviation of X_{sim} (simulated values) from X_{obs} (observed values) are the *RMSD* (root mean squared deviation) and the *MD* (or *bias*) (Kobayashi and Salam, 2000):

$$RMSD = \sqrt{\frac{1}{n}\sum_{i=1}^{n}(X_{obs} - X_{sim})^2} \quad (16)$$

$$MD = \frac{1}{n}\sum_{i=1}^{n}(X_{obs} - X_{sim}) \quad (17)$$

The *RMSD* represents the average distance between the simulated and observed values. The *MD* corresponds to the mean value of the differences between the simulated and observed values, although in this case negative differences are compensated by positive ones, which may lead to an erroneous interpretation. Both statistics represent different aspects of the deviation from simulated values, but the relationship between is not been well defined (Kobayashi and Salam, 2000).

The Nash-Sutcliffe efficiency (*NSE*) is a normalised statistic indicating the relative magnitude of the residual variance of the model ("noise") with respect to the variance of the observed values ("information") (Nash and Sutcliffe, 1970). The *NSE* indicates how well a plot of observed versus simulated values fits the 1:1 line (Moriase *et al*., 2007):

$$NSE = 1 - \left[\frac{\sum_{i=1}^{n}\left(X_{obs}-X_{sim}\right)^2}{\sum_{i=1}^{n}\left(X_{obs}-\overline{X}_{obs}\right)^2}\right] \quad (18)$$

where $\overline{X}_{obs}$ is the average value of all X_{obs} values. The *NSE* can take values between $-\infty$ and 1.0, the latter being the optimal value. Values between 0.0 and 1.0 are generally viewed as acceptable levels of performance (Moriase *et al*., 2007).

Percent bias (*PBIAS*) represents the mean trend of simulated values to greater or lower than their respective observed values (Gupta *et al*., 1999). The optimal value of *PBIAS* is 0.0, and values close to 0 indicate high model precision. Positive values indicate that the model provides values that are lower than those observed (model underestimation bias), whilst negative values indicate the opposite (model overestimation bias) (Gupta *et al*., 1999). *PBIAS* can be expressed as a percentage:

$$PBIAS = \left[\frac{\sum_{i=1}^{n}(X_{obs}-X_{sim})\times 100}{\sum_{i=1}^{n}(X_{obs})}\right] \quad (19)$$

RMSD-observations standard deviation ratio (*RSR*): this statistic standardises the values of *RMSD* with the standard deviation from the observed values (Moriasi *et al*., 2007). It combines both an error index and the additional information recommended by Legates and McCabe (1999):

$$RSR = \frac{RMSD}{STDEV_{obs}} = \left[\frac{\sqrt{\sum_{i=1}^{n}\left(X_{obs}-X_{sim}\right)^2}}{\sqrt{\sum_{i=1}^{n}\left(X_{obs}-\overline{X}_{obs}\right)^2}}\right] \quad (20)$$

RSR takes values from 0 to a large positive value, and when *RMSD* is equal to zero, the model is considered perfect. Small values of *RSR* indicate better performance of the simulation model (Moriasi *et al*., 2007).

3. ***Results and discussion***

Here, the results from the wind tunnel tests of the 35 insect-proof screens are presented. Two different models for estimating F_φ values as a function of different geometric screen characteristics are then presented, comparing the performance of these models with other models previously described in the literature. One model for estimating K_p values and another model for estimating Y values are presented and the performance of these models is compared with other models previously described in the literature. The effect of porosity on pressure drop predicted by the different models was analysed.

3.1. ***Aerodynamic characteristics assessed in wind tunnel tests***

Table 2 presents the values of the aerodynamic parameters (K_p, Y and F_φ) for the 35 insect-proof screens tested in a wind tunnel.

Table 2. Aerodynamic characteristics of the insect-proof screens: *a* and *b* are the coefficients of the polynomial fit from the wind tunnel tests (Eq. (2)); R^2, the fit determination coefficient; K_p, screen permeability [m^2]; Y, inertial factor; F_φ, pressure drop coefficient due to the presence of an insect-proof screen expressed as function of Re_p.

N: number of the screen.

N	*a*	*b*	R^2	K_p	Y	F_φ
1	2.784	3.045	0.9997	3.512×10^{-9}	0.233	$19.88\times(Re_p^{-1} + 0.233)$
2	2.102	2.676	0.9928	4.041×10^{-9}	0.187	$18.74\times(Re_p^{-1} + 0.187)$
3	2.036	2.253	0.9983	4.386×10^{-9}	0.206	$16.44\times(Re_p^{-1} + 0.206)$
4	2.407	2.876	0.9988	3.576×10^{-9}	0.212	$18.95\times(Re_p^{-1} + 0.212)$
5	1.767	1.676	0.9993	5.432×10^{-9}	0.216	$13.61\times(Re_p^{-1} + 0.216)$
6	3.029	3.792	0.9976	2.731×10^{-9}	0.231	$21.84\times(Re_p^{-1} + 0.231)$
7	2.985	3.235	0.9993	3.007×10^{-9}	0.254	$19.55\times(Re_p^{-1} + 0.254)$
8	1.519	1.534	0.9997	6.461×10^{-9}	0.186	$13.58\times(Re_p^{-1} + 0.186)$
9	1.879	3.074	0.9990	2.467×10^{-9}	0.186	$16.82\times(Re_p^{-1} + 0.186)$
10	1.909	2.375	0.9987	4.484×10^{-9}	0.181	$17.52\times(Re_p^{-1} + 0.181)$
11	1.845	1.876	0.9995	5.849×10^{-9}	0.194	$15.81\times(Re_p^{-1} + 0.194)$
12	1.852	1.899	0.9990	5.835×10^{-9}	0.193	$15.99\times(Re_p^{-1} + 0.193)$

13	1.947	2.176	0.9986	5.331×10^{-9}	0.185	$17.51\times(\mathrm{Re}_p^{-1} + 0.185)$
14	3.182	5.440	0.9992	1.716×10^{-9}	0.213	$24.83\times(\mathrm{Re}_p^{-1} + 0.213)$
15	3.595	6.006	0.9997	1.480×10^{-9}	0.235	$25.46\times(\mathrm{Re}_p^{-1} + 0.235)$
16	2.284	3.051	0.9994	3.211×10^{-9}	0.200	$19.05\times(\mathrm{Re}_p^{-1} + 0.200)$
17	0.870	2.635	0.9993	1.793×10^{-9}	0.118	$12.31\times(\mathrm{Re}_p^{-1} + 0.118)$
18	0.824	2.744	0.9992	1.713×10^{-9}	0.110	$12.51\times(\mathrm{Re}_p^{-1} + 0.110)$
19	2.235	4.738	0.9996	1.386×10^{-9}	0.192	$19.43\times(\mathrm{Re}_p^{-1} + 0.192)$
20	1.896	3.749	0.9997	1.798×10^{-9}	0.180	$17.52\times(\mathrm{Re}_p^{-1} + 0.180)$
21	1.575	3.179	0.9992	2.216×10^{-9}	0.159	$16.50\times(\mathrm{Re}_p^{-1} + 0.159)$
22	1.302	2.683	0.9993	2.745×10^{-9}	0.140	$15.50\times(\mathrm{Re}_p^{-1} + 0.140)$
23	1.261	2.645	0.9949	2.876×10^{-9}	0.134	$15.64\times(\mathrm{Re}_p^{-1} + 0.134)$
24	1.669	3.885	0.9995	1.853×10^{-9}	0.155	$18.20\times(\mathrm{Re}_p^{-1} + 0.155)$
25	2.562	4.159	0.9992	2.453×10^{-9}	0.187	$22.77\times(\mathrm{Re}_p^{-1} + 0.187)$
26	2.038	3.585	0.9994	2.028×10^{-9}	0.190	$17.84\times(\mathrm{Re}_p^{-1} + 0.190)$
27	1.913	1.844	0.9968	5.183×10^{-9}	0.218	$14.61\times(\mathrm{Re}_p^{-1} + 0.218)$
28	2.065	2.233	0.9949	3.926×10^{-9}	0.226	$15.33\times(\mathrm{Re}_p^{-1} + 0.226)$
29	3.886	5.802	0.9992	1.439×10^{-9}	0.269	$24.15\times(\mathrm{Re}_p^{-1} + 0.269)$
30	2.452	3.262	0.9992	3.154×10^{-9}	0.204	$20.10\times(\mathrm{Re}_p^{-1} + 0.204)$
31	5.872	6.111	0.9995	1.514×10^{-9}	0.377	$26.09\times(\mathrm{Re}_p^{-1} + 0.377)$
32	2.088	1.638	0.998	5.612×10^{-9}	0.255	$13.57\times(\mathrm{Re}_p^{-1} + 0.255)$
33	1.915	1.310	0.999	7.004×10^{-9}	0.266	$12.04\times(\mathrm{Re}_p^{-1} + 0.266)$
34	2.089	1.506	0.999	6.427×10^{-9}	0.260	$13.35\times(\mathrm{Re}_p^{-1} + 0.260)$
35	2.163	2.861	0.998	3.417×10^{-9}	0.199	$18.29\times(\mathrm{Re}_p^{-1} + 0.199)$

3.2. *Models for estimating F_φ values of an insect-proof screen with known geometric characteristics*

To study greenhouse microclimate using computational fluid dynamic (CFD) simulations or other types of mathematical simulation models it is necessary to know the aerodynamic characteristics of the screens. Typically, insect-proof screen manufacturers do not provide the aerodynamic characteristics or full geometric characteristics. Therefore, researchers often resort to models such as those presented in Eqs. (8), (9), (10), (14) and (15) to estimate the aerodynamic characteristics of the screens under study. For the screens analysed in this study, alternative models were developed for estimating the values of F_φ, K_p and Y from different geometric parameters.

From the F_φ expression determined using Eq. (6) (Table 2), F_φ values were calculated for each screen, at different values of airspeed u varying from 0.25 to 3.00 m s^{-1}, in +0.25 m s^{-1} intervals. The maximum limit was set to 3 m s^{-1} because this air velocity is unlikely to be reached in an insect-proof screen in a commercial greenhouse under natural ventilation conditions. The maximum values of air velocity observed near the vents of a commercial greenhouse with natural ventilation (side and roof vents) are normally unlikely to exceed 1.5 m s^{-1} (Molina-Aiz et al., 2009; López *et al*., 2012).

The first model, for estimating F_φ given the insect-proof screen porosity φ [m^2 m^{-2}] and using a Reynolds number Re_d based on the thread diameter D_h [m], is presented in the following equation derived from the experimental observations (Fig. 4b):

$$F_\varphi = \left(0.481002 + \frac{11.5331}{Re_d}\right)\left(\frac{1-\varphi^2}{\varphi^2}\right) \tag{21}$$

with a 0.97 correlation coefficient, with a 93.9% R^2 and with a p-value<0.001.

This equation is similar to those reported elsewhere in the literature where the value of F_φ is estimated from a thread diameter Reynolds number (similar to Eq. (11)).

The second model developed is useful for estimating F_φ when the thread diameter is difficult to assess. From the experimental data (Fig. 4a), the equation was derived for estimating F_φ from porosity φ [m^2 m^{-2}] and Reynolds number Re_t based on the screen thickness e [m] which is easier to measure with a micrometre:

$$F_\varphi = \left(0.475502 + \frac{26.2114}{Re_t}\right)\left(\frac{1-\varphi^2}{\varphi^2}\right) \tag{22}$$

This equation had a 0.96 correlation coefficient, with a 92.1% R^2 and with a p-value<0.001. The Reynolds based on screen thickness [m] is:

$$Re_t = \frac{e u \rho_a}{\mu} \tag{23}$$

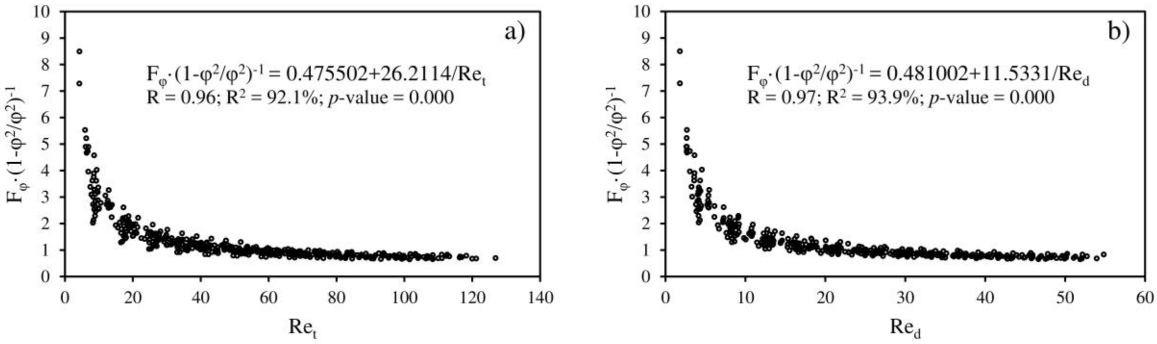

Fig. 4. Experimental $F_\varphi \cdot (1-\varphi^2/\varphi^2)^{-1}$ values expressed as a function of Re_t (a) and Re_d (b); the values of F_φ are calculated using Eq. (6).

Thus, Eqs. (21) and (22) allow values of F_φ exclusively to be estimated from geometric screen parameters and airspeed. Figure 5 shows the experimentally observed $F_{\varphi,obs}$ values calculated using Eq. [6] compared with $F_{\varphi,sim}$ values estimated using different models. For each screen presented in Table 1, and at different values of air velocity (u; ranging from 0.25 to 3.00 m s^{-1}, in intervals of +0.25 m s^{-1}), F_φ values were estimated using previously published Eqs. (8) (Hayama *et al*., 2000), Eq. (9) (Pinker and Herbert, 1967) and Eq. (10) (Bailey *et al*., 2003) and using models proposed in this study Eqs. (21) (with porosity and Reynolds number based on thread diameter Re_d) and Eq. (22) (with porosity and Reynolds number based on the screen thickness Re_t). This figure shows that the $F_{\varphi,sim}$ values estimated using Eqs. (21) and (22) proposed in this study fit the observed $F_{\varphi,obs}$ values better than the $F_{\varphi,sim}$ values estimated using Eqs. (8), (9) and (10).

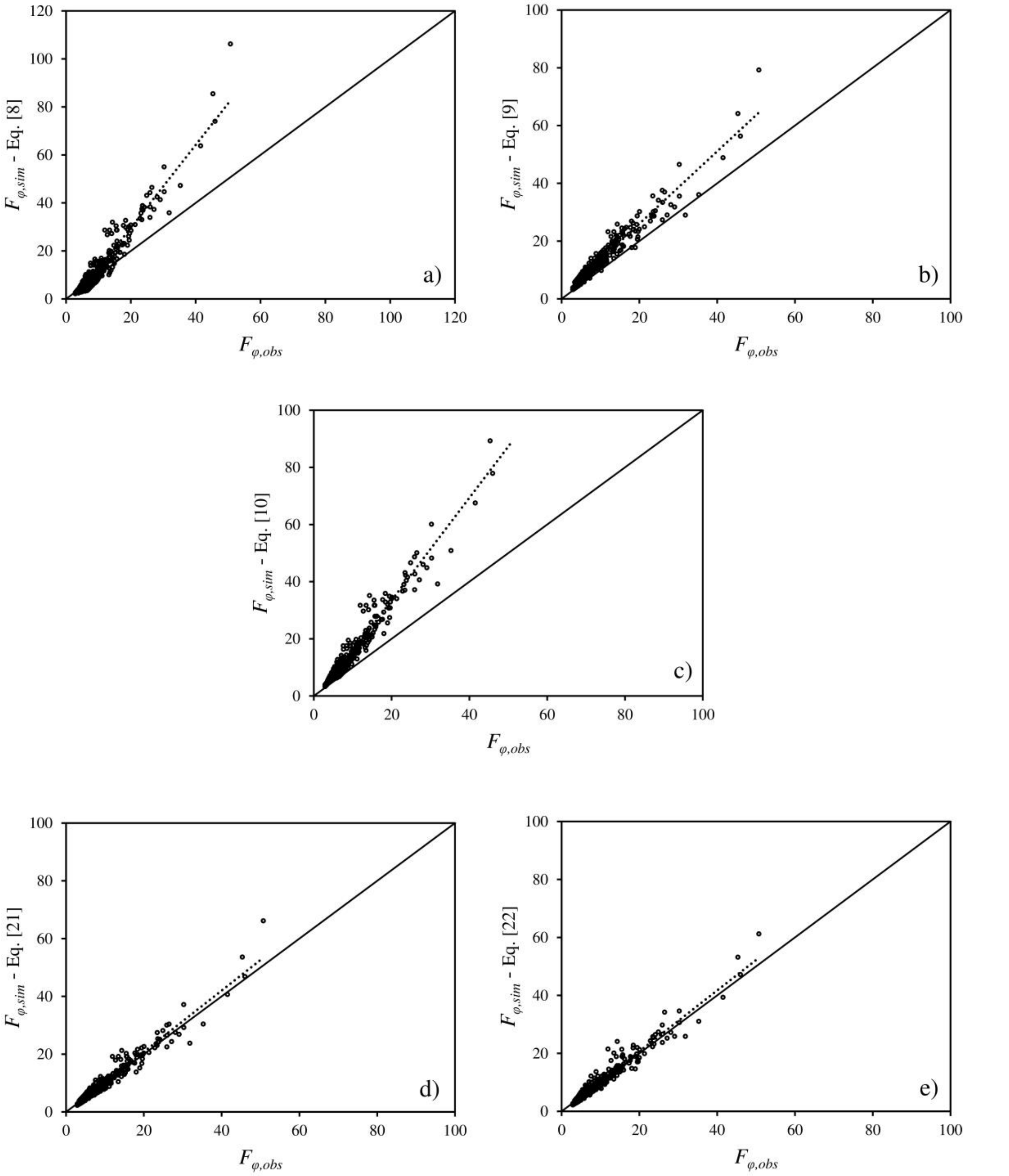

Fig. 5. F_φ values estimated using Eqs. (8) (a), (9) (b), (10) (c), (21) (d) and (22) (e) compared with experimental F_φ values (wind tunnel tests and with Eq. (6)).

Statistical analysis (Table 3) was also performed to identify the model for estimating $F_{\varphi,sim}$ that provides the values closest to the experimentally observed $F_{\varphi,obs}$ values. Both models presented in this study show significantly improved RMSD values with respect to models described in the literature, reaching values of 18.9% (Eq. (21)) and 19.1% (Eq. (22)). In this case, the NSE statistic reached 0.9 for Eqs. (21) and (22), almost equal to the optimal value, which is also an improvement when compared with other models described in the literature (Eqs. (8), (9) and (10)). The PBIAS statistic had negative values in the five models, which indicated that all models overestimated the value of F_{φ}, providing values higher than the experimentally observed values. However, the PBIAS values of the models presented in Eqs. (21) and (22) were very close to the optimal value of zero, in contrast to the other three models. The RSR values which can range from zero to ∞, were also improved by the models presented in Eqs. (21) and (22), with values closer to the optimal value of zero compared with the other models.

The results show that the models developed in this study (Eqs. (21) and (22)) provided $F_{\varphi,sim}$ values that fitted $F_{\varphi,obs}$ values better than the three models previously described in the literature. The first model, (Eq. (21)) required the same geometric parameters as the other models described in the literature; thus, to estimate F_{φ} values, the values of porosity and thread diameter for the screens must be known. Conversely, to apply the second model (Eq. (22)), the values of porosity and thickness of the screen must be known. This may be an advantage over the other models because the process to measure the thickness may be simpler than measuring thread diameter when it is not possible to obtain microscopic images. Measurement of the thread diameter with a micrometer is difficult because of the non-cylindrical shape of the thread as consequence of deformations that are produced during screen manufacture. However, the measurement of the screen thickness with a micrometer is simple and more exact.

Equation (8) by Hayama *et al*. (2000) was derived for wire nets; in this case, these authors worked with nine samples with 0.371, 0.504 and 0.778 porosity. The use of a metal wire net and only a small number of samples are possible reasons for Eq. (8) estimated F_{φ} with significant deviation from the experimentally observed values in our screen samples.

Equation (9), developed by Pinker and Herbert (1967) was derived originally using a small number of samples, with only 8 different samples of woven wire gauzes with porosity values ranging from 0.3 to 0.7 $m^2 m^{-2}$. These samples had a fabric structure similar to that of insect-proof screens. However, the material used (metal wire) was different from the polyethylene threads normally used today in insect-proof screens. These may be the reasons why this equation predicts F_φ values far from the experimentally observed values obtained here.

Equation (10), as used by Bailey *et al.* (2003), was derived by performing tests on 5 insect-proof screens with 0.25, 0.45, 0.53, 0.66 and 0.68 porosity. These porosity values are considerably different from the porosity values of the 35 screens used in this study, where porosity ranged from 0.237 to 0.556 $m^2 m^{-2}$. Of the 35 screens tested here, 29 had porosity values lower than 0.45 $m^2 m^{-2}$. This may explain why, that when using Eq. (10), the F_φ values assessed were also far from the experimentally observed values for our insect-proof screens.

Based on the findings of this study, it is recommended to apply an F_φ prediction equation that was derived using a sample of insect-proof screen as close to the example screen as possible.

Table 3. Statistical parameters of the comparison between experimentally observed $F_{\varphi,obs}$ values and $F_{\varphi,sim}$ values estimated using equations proposed in the literature: Eq. (8) (Hayama *et al.*, 2000), Eq. (9) (Pinker and Herbert, 1967) and Eq. (10) (Bailey *et al.*, 2003) along with the equations developed in this study: namely Eqs. (21) and (22), *R*, the correlation coefficient; *RMSD*, root mean squared error; *MD*, *bias*; *NSE*, the Nash-Sutcliffe efficiency; *PBIAS*, percent *bias*; *RSR*, *RMSD*-observations standard deviation ratio.

	Eq. (8)	**Eq. (9)**	**Eq. (10)**	**Eq. (21)**	**Eq. (22)**
R	0.970	0.974	0.979	0.970	0.960
RMSD	6.3	4.4	8.0	1.7	1.7
RMSD (%)	69.6	49.0	89.1	18.9	19.1
MD	-1.9	-3.7	-5.4	-0.2	-0.2
NSE	0.2	0.6	-0.3	0.9	0.9

PBIAS	-19.0	-36.1	-52.7	-1.6	-1.8
RSR	10.4	7.3	13.3	2.8	2.9

Conversely, in general, these equations for estimating F_φ values have a higher error in predicting F_φ for low air velocity values (Fig. 6). In the case of insect-proof screens, this is a serious drawback because the air velocity through these screens in a greenhouse with natural ventilation conditions is usually low, with maximum observed values of ~ 1.5 m s^{-1} (Molina-Aiz *et al.*, 2009; López *et* al., 2012). When using Eq. (8), 72% of the $F_{\varphi,sim}$ values have an error < 20% of the $F_{\varphi,obs}$ value. When using Eqs. (9) and (10), only 12% and 11% of the simulated values had an error < 20% of the $F_{\varphi,obs}$ value, respectively. However, when using Eqs. (21) and (22), proposed in this study, 94% and 92% of the $F_{\varphi,sim}$ values had an error < 20% of the $F_{\varphi,obs}$ value, respectively. Castellano *et al*. (2016) used equations similar to those used here to predict the aerodynamic characteristics of insect-proof screens with satisfactory results, but these authors performed tests in a wind tunnels using air velocities >4 m s^{-1}.

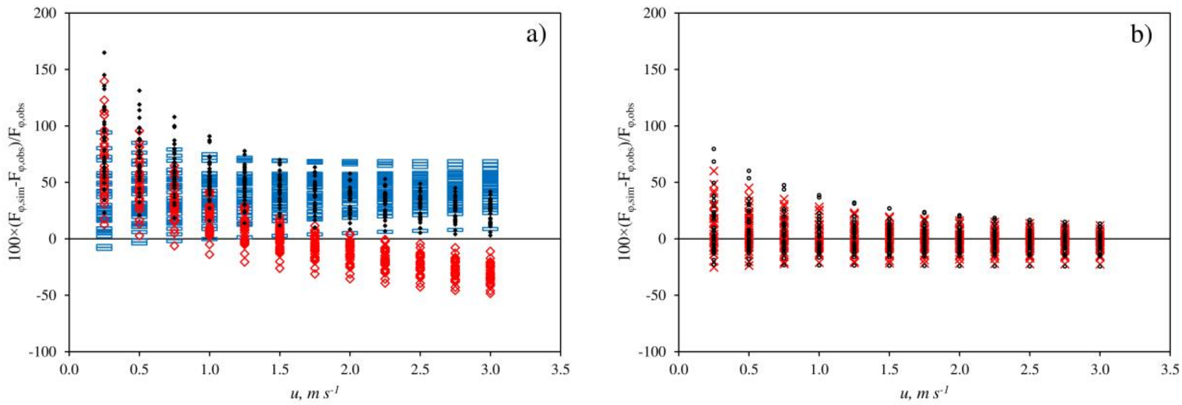

Fig. 6. Error observed between $F_{\varphi,obs}$ and $F_{\varphi,sim}$ (%) as a function of the air velocity. (a) $F_{\varphi,sim}$ assessed using Eq. (8) (◊) (Hayama *et al*., 2000), Eq. (9) (═)(Pinker and Herbert, 1967), [10] (♦) (Bailey *et al*., 2003). (b) $F_{\varphi,sim}$ assessed using Eqs. (21) (×) and (22) (○).

3.3. *Models for estimating K_p and Y values of an insect-proof screen given their geometric characteristics*

Another option for the aerodynamic characterisation of an insect-proof screen is to use the screen permeability K_p and its inertial factor Y. Given these parameters, curves of pressure drop as a function of air velocity of a screen can be constructed by applying the modified Darcy's equation (Forchheimer, 1901), indicated in Eq. (1). These two parameters (Table 2) were determined in wind tunnel tests for the 35 study screens. Previously, Miguel (1998) presented two models for estimating the value of these two parameters from screen porosity (Eqs. (14) and (15)). The constants β, A and B, in Eqs. (12) and (13) presented by Nield and Bejan (1999) were also determined statistically for the 35 screens analysed in this study. This led to the following equation for estimating the screen permeability K_p (β=2.0679) with the thread diameter D_h [m] and porosity [m^2 m^{-2}]:

$$K_p = \frac{{D_h}^2 \varphi^3}{2.0679(1-\varphi)^2} + 3.8362 \times 10^{-10} \quad (24)$$

with 0.75 correlation coefficient, a 56.3% R^2 and a p-value < 0.05. The following equation can be used to estimate the inertial factor Y of the screen (A = 0.0571195 and B = 0.135966) with the thread diameter [m] and the diameter of the inside circumference of the pore D_i [m]:

$$Y = 0.0571195 + 0.135966 \frac{D_h}{D_i} \quad (25)$$

with a 0.76 correlation coefficient, a 58.1% R^2 and a p-value < 0.0001.

Figure 7 shows the values of K_p (a) and Y (b) estimated using the Eqs. (14) and (15) as a function only of screen porosity proposed by Miguel (1998) and the Eqs. (24) and (25) obtained in this study in the way proposed by Nield and Bejan (1999) as a function of porosity and geometric characteristics of the screens, all of which are represented with respect to the experimentally observed values (Table 2). This figure shows that the inertial factor (Y) values derived using the equations by Miguel (1998) are much higher than the experimentally observed values and that the permeability (K_p) values are much lower than the experimentally observed values. With

Eqs. (24) and (25) derived from the geometric characteristics of the screen as suggested by Nield and Bejan (1999), the values similarly approximate the experimentally observed values.

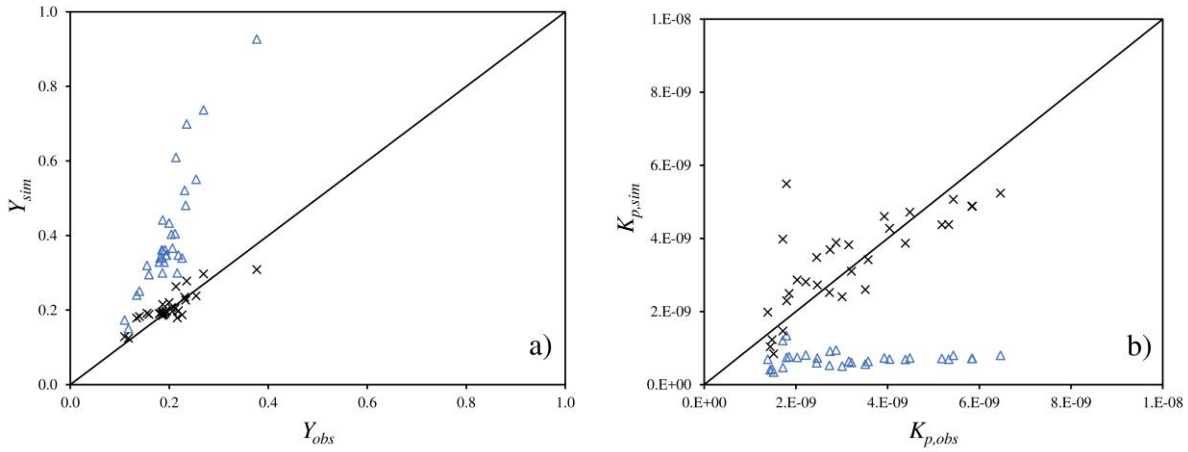

Fig. 7. Simulated *Y* (a) and K_p (b) values compared to experimentally observed values. (Δ), Eqs. (14) and (15) proposed by Miguel (1998); (×), Eqs. (26) and (27) derived from the geometric characteristics of the screens.

Statistical analysis was also performed (Table 4) to identify the equation(s) for estimating the K_p and *Y* values that provide the closest simulated values to the experimentally observed values. The equations proposed by Miguel (1998) for estimating the K_p and *Y* values provide values very far from the experimentally observed values (Fig. 7 and Table 4). Therefore, in principle, we advise against using these equations for several reasons. Miguel (1998) when developing the model used only 14 screens. In addition, different types of screens were combined, 8 screens with rectangular pores, similar to the screens used in this study, and 6 shade screens with irregular pores made of a different type of fabric. Conversely, the equations of this study (Eqs. (24) and (25)) were derived using more screens (35 in number), all of which were the same type of fabric (weft and warp) with rectangular pores and with a narrow porosity range, from 0.237 to 0.556 m^2 m^{-2}.

Based on the results, Eqs. (24) and (25) should be used to estimate K_p and Y values, in preference to the equations proposed by Miguel (1998) as a function of only the screen porosity. Equations (24) and (25), however, require knowledge of the thread diameter, the inner pore diameter and the porosity. Also, the screen thickness e must also be known to apply Eq. (1) and thus construct the pressure drop curve for the screen. In CFD software, a porous jump boundary conditions can be used to model screens (Molina-Aiz *et al*., 2017) and filters knowing values of K_p, Y and e.

Table 4. Statistical parameters of the comparison between the experimentally observed $K_{p,obs}$ and Y_{obs} values and the $K_{p,sim}$ and Y_{sim} values estimated using the Eq. (14) and (15) (Miguel, 1998) proposed in the literature and Eqs. (24) and (25) based on the model proposed by Nield and Bejan (1999); *RMSD*, root mean squared error; *MD*, *bias*; *NSE*, the Nash-Sutcliffe efficiency; *PBIAS*, percent *bias*; *RSR*, *RMSD*-observations standard deviation ratio.

	K_p		Y	
	Eq. (14)	**Eq. (24)**	**Eq. (15)**	**Eq. (25)**
R	0.063	0.750	0.798	0.763
RMSD	3.240×10^{-9}	1.100×10^{-9}	0.220	0.025
RMSD (%)	92.9	31.5	107.9	12.1
MD	7.058×10^{-10}	3.487×10^{-9}	0.396	0.204
NSE	-2.8	0.6	-22.2	0.7
PBIAS	79.8	0.0	-87.1	-2.7
RSR	1.933×10^{-4}	6.561×10^{-5}	2.5	0.3

3.4. Effect of porosity in the pressure drop estimation with the different models for calculate F_φ, K_p and Y

For the 35 screens (Table 1) and with the different values of F_φ, estimated using Eqs. (8) from Hayama *et al*. (2000), (9) from Pinker and Herbert (1967) and (10) from Bailey *et al*. (2003) along with Eqs. (21) and (22) derived from the present study, Eq. (5) can be used to obtain the values of pressure drop as a function of air velocity. In the same way, with the values of K_p and

Y estimated using Eqs. (14) and (15) (Miguel, 1998) and Eqs. (24) and (25) derived from this work from the general equations used for porous media (Nield and Bejan, 1999), Eq. (1) can be applied to obtain the values of pressure drop as a function of air velocity. Figure 8 shows the error (%) between the pressure drops measured in the wind tunnel ΔP_{obs} and those calculated from the different equations ΔP_{sim} as a function of the screen porosity. In Fig. 8a the error obtained with previous models of the pressure drop coefficient F_{φ} found in the literature is shown. In Fig. 8b the error obtained with the different models (two for F_{φ} and one using K_p and Y) can be seen.

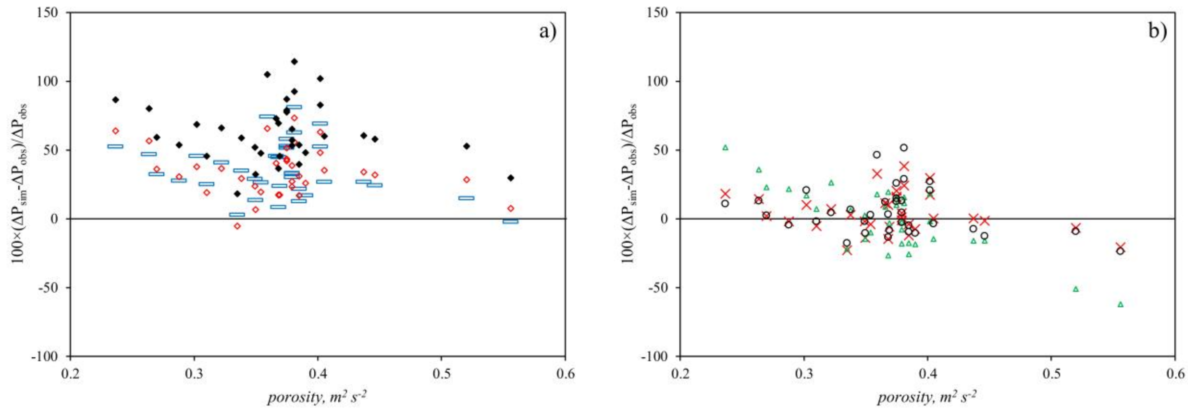

Fig. 8. Average error observed between ΔP_{obs} and ΔP_{sim} (%), for air velocities from 0.25 to 1.25 m s^{-1}, as a function of the porosity of the screens. (a) ΔP_{sim} estimated using Eq. (8) (◊) from Hayama *et al*. (2000), Eq. (9) (=) from Pinker and Herbert (1967), Eq. (10) (♦) from Bailey *et al*. (2003). (b) ΔP_{sim} estimated using Eq. (21) (×), Eq. (22) (○) and Eqs. (24) and (25) (Δ).

In general, the pressure drops calculated from models of F_{φ} obtained from the literature overestimated the measured values for all porosities ranging from 0.24 to 0.56 (Fig. 8a). The average errors for all porosities and velocities lower than 1.25 m s^{-1} were 34.7% for Eq. (8), from Hayama *et al*. (2000), 35.5% for Eq. (9) from Pinker and Herbert (1967) and 63.3% for Eq. (10) from Bailey *et al*. (2003). However, the errors of the purposed models of F_{φ}, derived from porosity and the Re number obtained with the thread diameter (Eq. (21)) and the screen thickness (Eq. (22)), appear to be uniform as a function of screen porosity, with average values of 5.2% and 4.4%, respectively.

Using the values of aerodynamic properties of the screens (permeability K_p and inertial factor Y) calculated with Eqs. (24) and (25), derived from porosity and two geometric characteristics of the screen (D_h and D_i), the average error was zero as consequence of an overestimation for porosities lower than 0.3 and underestimation for porosities greater than 0.5 (Fig. 8b).

Figure 9 shows the error (%) between pressure drop measured experimentally in the wind tunnel ΔP_{obs} and the pressure drop ΔP_{sim} calculated with the values of K_p and Y estimated using Eqs. (14) and (15) (Miguel, 1998) and Eqs. (24) and (25) derived from parameters presented by Nield and Bejan (1999). In Fig. 9 it can be seen how the models presented by Miguel (1998) provide a much higher error than the models obtain in this work for porosities < 0.5, and similar errors for the two screens with porosities between 0.5 and 0.6.

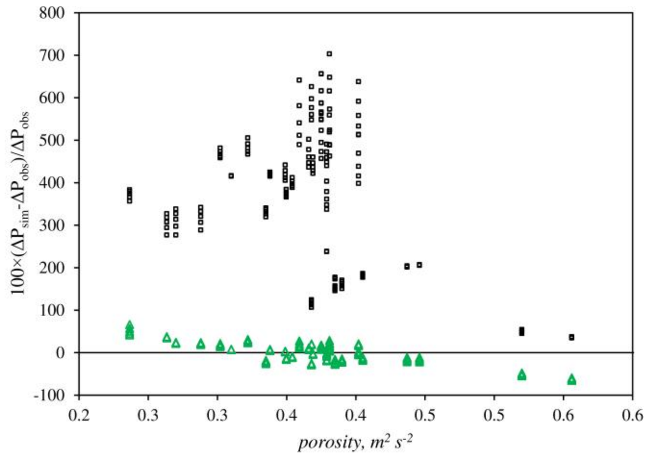

Fig. 9. Error observed between pressure drop measured experimentally in the wind tunnel ΔP_{obs} and calculated ΔP_{sim} (%) as a function of the porosity of the screens. ΔP_{sim} estimated using Eqs. (14) and (15) proposed by Miguel (1998) (□) and Eqs. (26) and (27) derived from parameters presented by Nield and Bejan (1999) (△), using air velocities u ranging from 0.25 to 1.25 m s^{-1}, in +0.25 m s^{-1} intervals).

The errors of Figs. 8 and 9 correspond to the models obtained with new insect-proof screens that have never been installed in a greenhouse. Once installed in the vents of the greenhouse, and with the passage of time, the screens deteriorate and this can cause the screen fto become less rigid, increasing in thickness and reducing pressure drop (López *et al*., 2018). On the other hand, the accumulation of dirt causes an important increases of F_φ (between 16.5% and 61.2%; for u=1.0 m s^{-1}) and consequently increases in pressure drop (López *et al*., 2018). These contrary effects of material ageing and dirt accumulation on the aerodynamic characteristics of screens must also be taken into account when applying the models described here.

4. *Conclusions*

Different models for estimating the aerodynamic characteristics of insect-proof screens, with a weft and warp fabric, using one or more geometric parameters, were presented and validated in this study. These models were generated from data obtained from 35 insect-proof screens with porosity ranging from 0.237 to 0.556 m^2 m^{-2}.

Two options were validated for estimating the pressure drop coefficient F_φ: the first model was based on the screen porosity and a Reynolds number based on thread diameter and the second model was based on the screen porosity and a Reynolds number based on thickness.

A third option was based on estimating the permeability K_p and the inertial factor Y. Two equations were obtained for estimating the value of K_p as a function of thread diameter D_h and porosity φ and for estimating the value of Y as a function of thread diameter and the inner pore diameter D_i. These models have been shown to improve the accuracy of the previous models described in literature that overestimated the pressure drops for all porosities analysed.

Models for aerodynamic parameters of the insect-proof screens K_p and Y based in their geometric characteristics are very important to simulate the effect of this porous media in CFD studies. Knowledge of K_p, Y and thickness allows to model insect-proof screens in CFD simulations as a thin membrane using the porous jump model applied to a face zone.

Future studies should be orientated towards the development of more robust models and it would be interesting to increase the porosity range and evaluate lower air velocities.

5. *Acknowledgements*

This work has been funded by the Spanish Ministry of Economy and Competitiveness and the European Regional Development Fund (ERDF) by means of the research grant AGL2015-68050-R. The authors wish to express their gratitude to the Research Centre CIAIMBITAL of the University of Almería (Spain) for their support throughout the development of this study.

6. *References*

Álvarez, A.J. (2010). *Estudio de las características geométricas y del comportamiento aerodinámico de las mallas antiinsectos utilizadas en los invernaderos como medida de protección vegetal*. PhD thesis. Almería, Spain: University of Almería, p. 423.

Álvarez, A. J., Oliva, R. M. & Valera, D. L. (2012). Software for the geometric characterisation of insect-proof screens. *Computers and Electronics in Agriculture*, 82, 134–144. [DOI: http://dx.doi.org/10.1016/j.compag.2012.01.001]

Bailey, B. J., Montero, J. I., Pérez Parra, J., Robertson, A. P., Baeza, E. & Kamaruddin, R. (2003). Airflow resistance of greenhouse ventilators with and without insect screens. *Biosystems Engineering*, 86(2), 217–229. [DOI: https://doi.org/10.1016/S1537-5110(03)00115-6]

Bartzanas, T., Boulard, T. & Kittas, C. (2002). Numerical simulation of the airflow and temperature distribution in a tunnel greenhouse equipped with insect-proof screen in the openings. *Computers and Electronics in Agriculture*, 34, 207–221. [DOI: https://doi.org/10.1016/S0168-1699(01)00188-0]

Berlinger, M. J., Leblush-Mordechl, S., Fridja, D. & Mor, N. (1993). The effect of types of greenhouse screens on the presence of western flower thrips: a preliminary study. *IOBC/WPRS*

Bulletin, 16(2), 13–16. [avalaible online: http://library.wur.nl/WebQuery/titel/843670 (accessed on 1 June 2019)]

Beavers, G. S., Sparrow, E. M. & Rodenz, D. E. (1973). Influence of Bed Size on the Flow Characteristics and Porosity of Randomly Packed Beds of Spheres. *Journal of Applied Mechanics*, 40 (3), 655–660. [DOI: http://dx.doi.org/10.1115/1.3423067]

Castellano, S. Starace, G., De Pascalis, L., Lippolis, M. & Mugnozza, G. S. (2016). Test results and empirical correlations to account for air permeability of agricultural nets. *Biosystems Engineering*, 150, 131–141. [DOI: http://dx.doi.org/10.1016/j.biosystemseng.2016.07.007]

Dierickx, I. E. (1998). Flow reduction of synthetic screens obtained with both a water and airflow apparatus. *Journal of Agricultural Engineering Research*, 71, 67–73. [DOI: http://dx.doi.org/10.1006/jaer.1998.0299]

Espinoza, K., Valera, D. L., Torres, J. A., López, A. & Molina-Aiz, F. D. (2015). An Auto-Tuning PI Control System for an Open-Circuit Low-Speed Wind Tunnel Designed for Greenhouse Technology. *Sensors*, 15, 19723–19749. [DOI: http://dx.doi.org/10.3390/s150819723]

Fatnassi, H., Boulard, T., Demrati, H., Bouirden, L. & Sappe, G. (2002). Ventilation Performance of a Large Canarian-Type Greenhouse equipped with Insect-proof Nets. *Biosystems Engineering*, 82(1), 97–105. [DOI: http://dx.doi.org/10.1006/bioe.2001.0056]

Fatnassi, H., Boulard, T. & Bouirden, L. (2003). Simulation of climatic conditions in full-scale greenhouse fitted with insect-proof screens. *Agricultural and Forest Meteorology*, 118, 97–111. [DOI: https://doi.org/10.1016/S0168-1923(03)00071-6]

Fatnassi, H., Boulard, T., Poncet, C. & Chave, M. (2006). Optimisation of greenhouse insect screening with computational fluid dynamics. *Biosystems Engineering*, 93(3), 301–312. [DOI: https://doi.org/10.1016/j.biosystemseng.2005.11.014]

Forchheimer, P. (1901). Wasserbewegung durch Boden [Water movement from ground]. *Zeitschrift des Vereines Deutscher Ingenieure*, 45, 1782–1788.

Gupta, H. V., Sorooshian, S. & Yapo, P. O. (1999). Status of automatic calibration for hydrologic models: Comparison with multilevel expert calibration. *Journal of Hydrologic Engineering*, 4(2), 135–143. [DOI: https://doi.org/10.1061/(ASCE)1084-0699(1999)4:2(135)]

Harmanto, Tantau, H. J. & Salokhe, V. M., 2006. Microclimate and air exchange rates in greenhouses covered with different nets in the humid tropics. *Biosystems Engineering*, 94(2), 239–253. [DOI: https://doi.org/10.1016/j.biosystemseng.2006.02.016]

Hayama, S., Peng, G. & Ishizuka, M. (2000). Measurement of flow resistance coefficients for wire nets in natural air convection flow. Proc. *Sixth Triennal International Symposium on Fluid Control, Measurement and Visualization* (FLUCOME 2000), Sherbrooke, Canada, 13-17 August, 12 pp. [Avalaible online: https://www.tib.eu/en/search/id/BLCP%3ACN071523984/Measurement-of-Flow-Resistance-Coefficients-for/ (accessed on 1 june 2019)]

Kittas, C., Boulard, T., Bartzanas, T., Katsoulas, N. & Mermier, M. (2002). Influence of an insect screen on greenhouse ventilation. *Transactions of the ASAE*, 45(4), 1083–1090. [DOI: http://dx.doi.org/10.13031/2013.9940]

Kittas, C., Katsoulas, N., Bartzanas, T., Mermier, M. & Boulard, T. (2008). The impact of insect screens and ventilation openings on the greenhouse microclimate. *Transactions of the ASABE*, 51(6), 2151–2165. [DOI: http://dx.doi.org/10.13031/2013.25396]

Kobayashi, K. & Salam, M. U. (2000). Comparing simulated and measured values using mean squared deviation and its components. *Agronomy Journal*, 92, 345–352. [DOI: doi: https://doi.org/10.2134/agronj2000.922345x]

Kosmos, S. R., Riskowski, G. L. & Christianson, L. L. (1993). Force and static pressure resulting from airflow through screens. *Transactions of the ASAE*, 36(5), 1467–1472. [DOI: http://dx.doi.org/10.13031/2013.28487]

Legates, D. R. & McCabe, G. J. (1999). Evaluating the use of "goodness-of-fit" measures in hydrologic and hydroclimatic model validation. *Water Resources Research*, 35(1), 233–241. [DOI: https://doi.org/10.1029/1998WR900018]

Linker, R., Tarnopolsky, M. & Seginer, I. (2002). Increased resistance to flow and temperature-rise resulting from dust accumulation on greenhouse insect-proof screens. *ASAE Annual International Meeting*, Chicago (USA), Jun 28-31, 9 pp. [DOI: http://dx.doi.org/10.13031/2013.10475]

López, A., Valera, D. L., Molina-Aiz, F. D. & Peña, A. (2012). Sonic anemometry measurements to determine airflow patterns in multi-tunnel greenhouse. *Spanish Journal of Agricultural Research*, 10(3), 631–642. [DOI: http://dx.doi.org/10.5424/sjar/2012103-660-11]

López, A., Valera, D. L., Molina-Aiz, F. D., Peña, A. & Marín, P. (2013). Field analysis of the deterioration after some years of use of four insect-proof screens utilized in Mediterranean greenhouses. *Spanish Journal of Agricultural Research*, 11(4), 958–967. [DOI: http://dx.doi.org/10.5424/sjar/2013114-4093]

López, A., Valera, D. L., Molina-Aiz, F. D., Peña A. & Marín, P. (2014). Microclimate evaluation of a new design of insect-proof screens in a Mediterranean greenhouse. *Spanish Journal of Agricultural Research*, 12(2), 338–352. [DOI: http://dx.doi.org/10.5424/sjar/2014122-4956]

López, A., Molina-Aiz, F. D., Valera, D. L., Peña, A. & Espinoza, K. (2018). Effect of material ageing and dirt on the behaviour of greenhouse insect-proof screens. *Spanish Journal of Agricultural Research*, 16(4), e0205, 12 pages. [DOI: https://doi.org/10.5424/sjar/2018164-11711]

Miguel, A. F. (1998). Airflow through porous screens: from theory to practical considerations. *Energy and Buildings*, 28, 63–69. [DOI: https://doi.org/10.1016/S0378-7788(97)00065-0]

Miguel, A. F. & Silva, A. M. (2000). Porous materials to control climate behaviour of enclosures: an application to the study of screened greenhouses. *Energy and Buildings*, 31, 195–209. [DOI: https://doi.org/10.1016/S0378-7788(99)00010-9]

Miguel, A. F., Van de Braak, N. J. & Bot, G. P. A. (1997). Analysis of the airflow characteristics of greenhouse screening materials. *Journal of Agricultural Engineering Research*, 67, 105–112. [DOI: http://dx.doi.org/10.1006/jaer.1997.0157]

Molina-Aiz, F. D., Valera, D. L. & Álvarez, A. J. (2004). Measurement and simulation of climate inside Almería-type greenhouses using computational fluid dynamics. *Agricultural and Forest Meteorology*, 125, 33–51. [DOI: http://dx.doi.org/10.1016/j.agrformet.2004.03.009]

Molina-Aiz, F. D., Valera, D. L., Álvarez, A. J. & Madueño, A. (2006). A wind tunnel study of airflow through horticultural crops: determination of the drag coefficient. *Biosystems Engineering*, 93(4), 447–457. [DOI: http://dx.doi.org/10.1016/j.biosystemseng.2006.01.016]

Molina-Aiz, F. D., Valera, D. L., Peña, A. A., Gil, J. A. & López, A. (2009). A Study of Natural Ventilation in an Almería-Type Greenhouse with Insect Screens by Means of Tri-sonic Anemometry. *Biosystems Engineering*, 104, 224–242. [DOI: https://doi.org/10.1016/j.biosystemseng.2009.06.013]

Molina-Aiz, F. D., Norton, T., López, A., Reyes-Rosas, A., Moreno, M.A., Marín, P., Espinoza, K. & Valera, D. L. (2017). Using Computational Fluid Dynamics to analyse the CO_2 transfer in naturally ventilated greenhouses. *Acta Horticulturae*, 1182, 283–292. [DOI: https://doi.org/10.17660/ActaHortic.2017.1182.34]

Montero, J. I., Muñoz, P. & Antón, A. (1997). Discharge coefficients of greenhouse windows with insect-proof screens. *Acta Horticulturae*, 443, 71–77. [DOI: http://dx.doi.org/10.17660/ActaHortic.1997.443.8]

Moriasi, D. N., Arnold, J. G., Van Liew, M. W., Bingner, R. L., Harmel, R. D. & Veith, T. L. (2007). Model evaluation guidelines for systematic quantification of accuracy in watershed simulations. *Transactions of the ASABE*, 50(3), 885−900. [DOI: https://doi.org/10.13031/2013.23153]

Muñoz, P., Montero, J. I., Antón, A. & Giuffrida, F., 1999. Effect of insect-proof screens and roof openings on greenhouse ventilation. *Journal of Agricultural Engineering Research*, 73, 171–178. [DOI: http://dx.doi.org/10.1006/jaer.1998.0404]

Nash, J. E. & Sutcliffe, J. V. (1970). River flow forecasting through conceptual models: Part 1. A discussion of principles. *Journal of Hydrology*, 10(3), 282–290. [DOI: https://doi.org/10.1016/0022-1694(70)90255-6]

Nield, D. A. & Bejan, A. (1999). *Convection in porous media*. (2nd ed.) New York: Springer.

Pinker, R. A. & Herbert, M. V. (1967). Pressure loss associated with compressible flow through square-mesh wire gauzes. *Journal of Mechanical Engineering Science*, 9(1), 11–23. [DOI: https://doi.org/10.1243%2FJMES_JOUR_1967_009_004_02]

Soni, P., Salokhe, V. M. & Tantau, H. J. (2005). Effect of Screen Mesh Size on Vertical Temperature Distribution in Naturally Ventilated Tropical Greenhouses. *Biosystems Engineering*, 92(4), 469–482. [DOI: http://dx.doi.org/10.1016/j.biosystemseng.2005.08.005]

Taylor, R. A. J., Shalhevet, S., Spharim, I., Berlinger, M. J. & Lebiush-Mordechi, S. (2001). Economic evaluation of insect-proof screens for preventing tomato yellow leaf curl virus of tomatoes in Israel. *Crop Protection*, 20, 561–569. [DOI: https://doi.org/10.1016/S0261-2194(01)00022-9]

Teitel, M. (2001). The effect of insect-proof screens in roof openings on greenhouse microclimate. *Agricultural and Forest Meteorology*, 110, 13–25. [DOI: http://dx.doi.org/10.1016/S0168-1923(01)00280-5]

Teitel, M. (2007). The effect of screened openings on greenhouse microclimate. *Agricultural and Forest Meteorology*, 143(3–4), 159–175. [DOI: http://dx.doi.org/10.1016/j.agrformet.2007.01.005]

Teitel, M. (2010). Using computational fluid dynamics simulations to determine pressure drops on woven screens. *Biosystems Engineering*, 105, 172–179. [DOI: http://dx.doi.org/10.1016/j.biosystemseng.2009.10.005]

Teitel, M. & Shklyar, A. (1998). Pressure drop across insect-proof screens. *Transactions of the ASAE*, 41(6), 1829–1834. [DOI: http://dx.doi.org/10.13031/2013.17336]

Valera, D. L., Álvarez, A. J. & Molina-Aiz, F. D. (2006). Aerodynamic analysis of several insect-proof screens used in greenhouses. *Spanish Journal of Agricultural Research*, 4(4), 273–279. [DOI: http://doi.org/10.5424/sjar/2006044-204]

Valera, D. L., Belmonte, L. J., Molina-Aiz, F. D. & López, A. (2016). *Greenhouse Agriculture in Almería. A Comprehensive Techno-Economic Analysis*. (1st ed). Almería (Spain): Cajamar Caja Rural. [Available online: http://www.publicacionescajamar.es/series-tematicas/economia/greenhouse-agriculture-in-almeria-a-comprehensive-techno-economic-analysis/ (accessed on 1 June 2019)]

Figure

Click here to access/download;Figure;Figure 1.tif

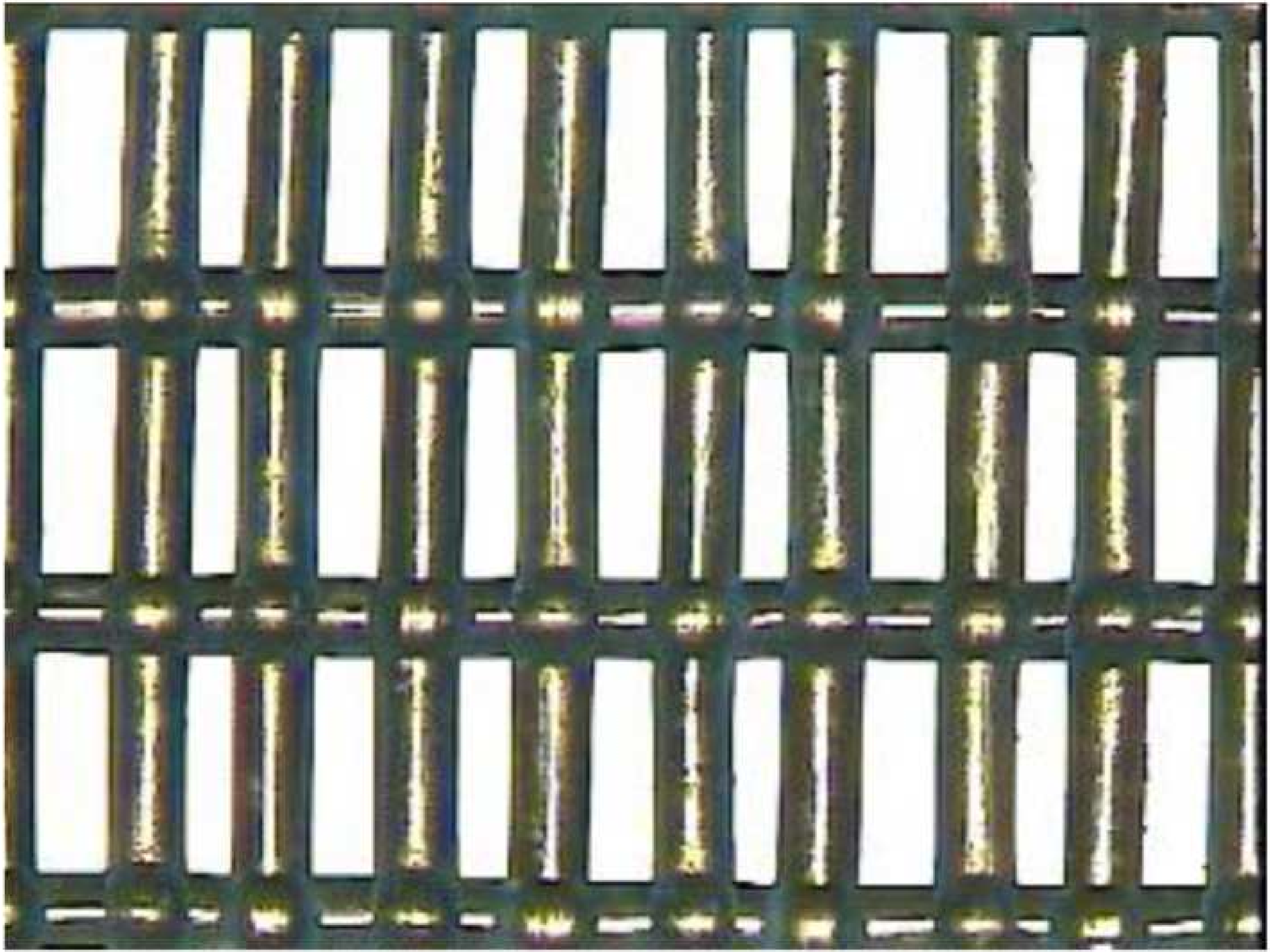

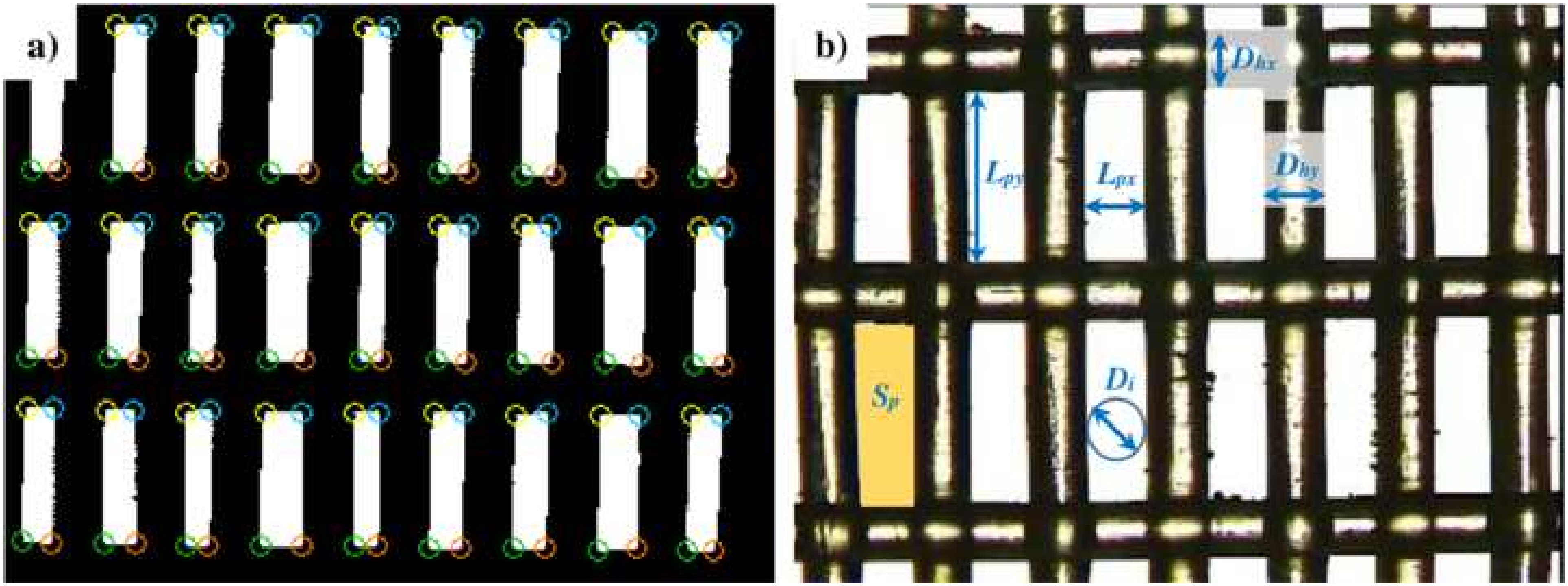
a)
b)
Dhx
Lpy
Lpx
Dhy
Sp
Dl

Figure

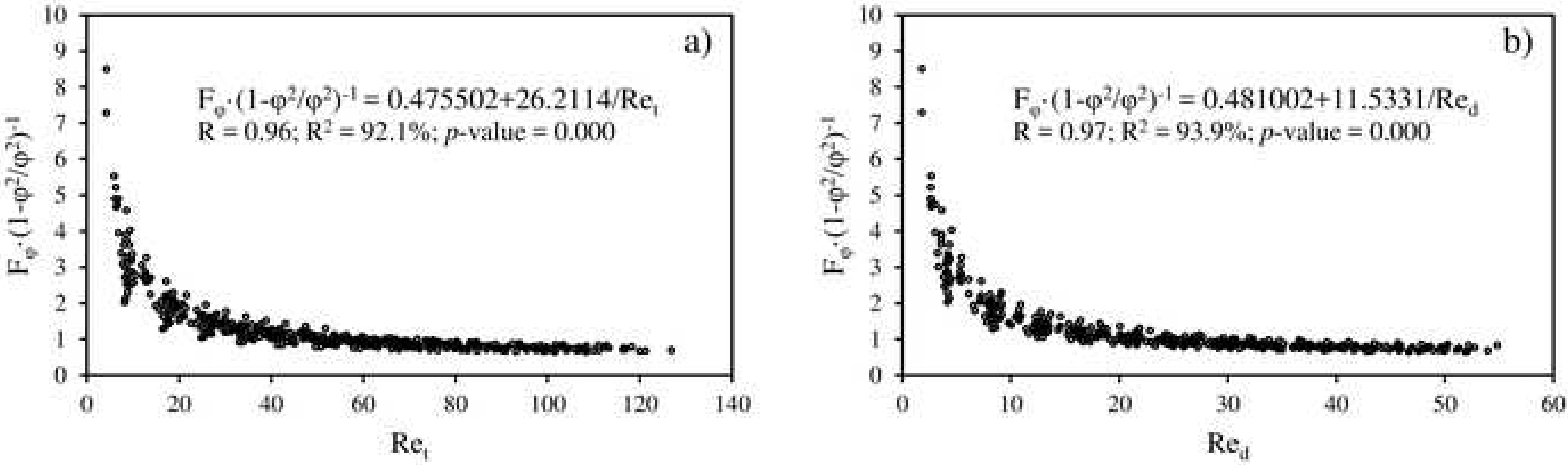
a)
$F_\varphi \cdot (1-\varphi^2/\varphi^2)^{-1}$ = 0.475502+26.2114/Re_t
R = 0.96; R^2 = 92.1%; p-value = 0.000
$F_\varphi \cdot (1-\varphi^2/\varphi^2)^{-1}$
Re_t
0
20
40
60
80
100
120
140
0
1
2
3
4
5
6
7
8
9
10
b)
$F_\varphi \cdot (1-\varphi^2/\varphi^2)^{-1}$ = 0.481002+11.5331/Re_d
R = 0.97; R^2 = 93.9%; p-value = 0.000
$F_\varphi \cdot (1-\varphi^2/\varphi^2)^{-1}$
Re_d
0
10
20
30
40
50
60

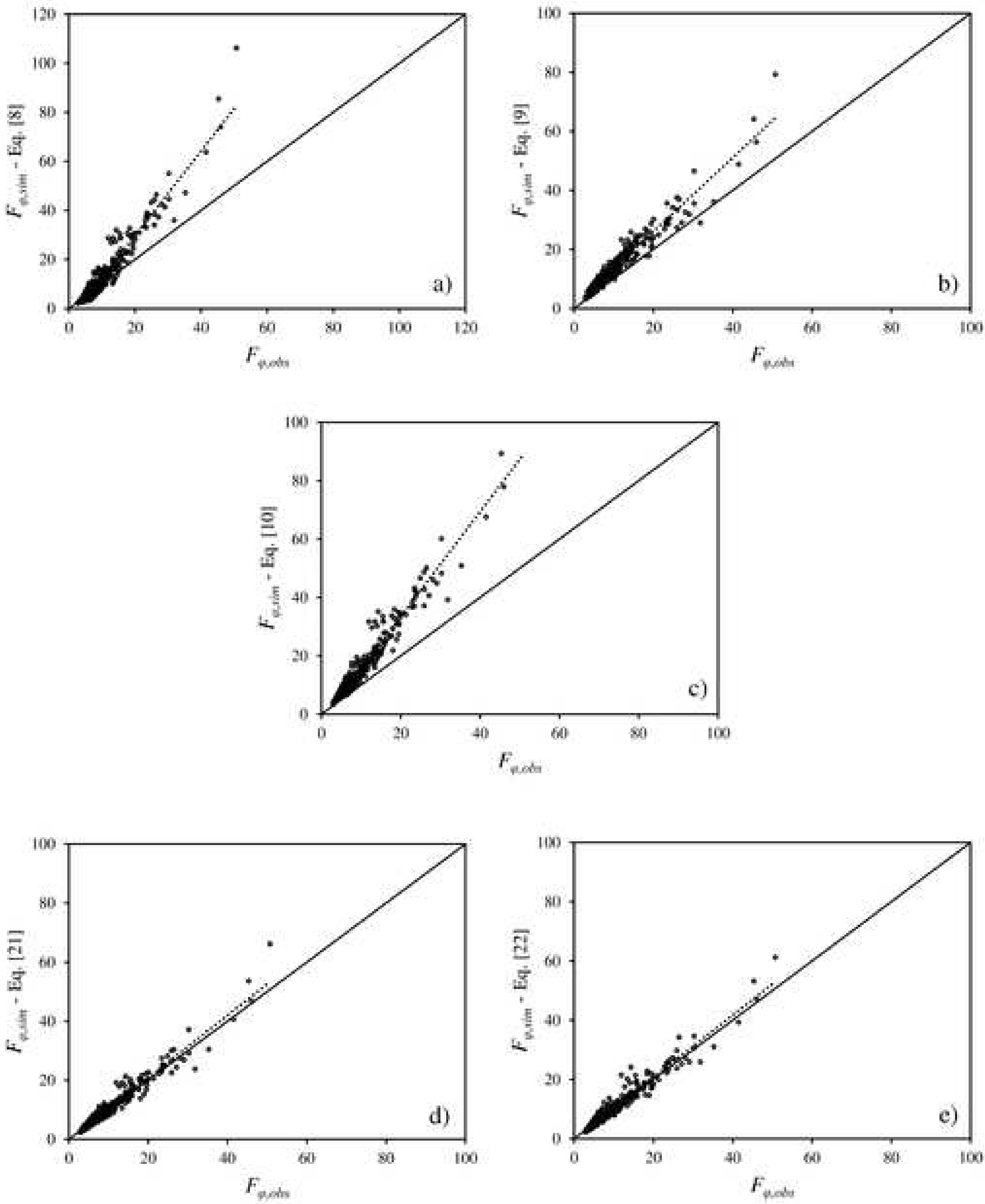

$F_{\varphi,sim}$ - Eq. [8]
$F_{\varphi,obs}$
a)
$F_{\varphi,sim}$ - Eq. [9]
$F_{\varphi,obs}$
b)
$F_{\varphi,sim}$ - Eq. [10]
$F_{\varphi,obs}$
c)
$F_{\varphi,sim}$ - Eq. [21]
$F_{\varphi,obs}$
d)
$F_{\varphi,sim}$ - Eq. [22]
$F_{\varphi,obs}$
e)

Figure

Click here to access/download;Figure;Figure 6.jpg

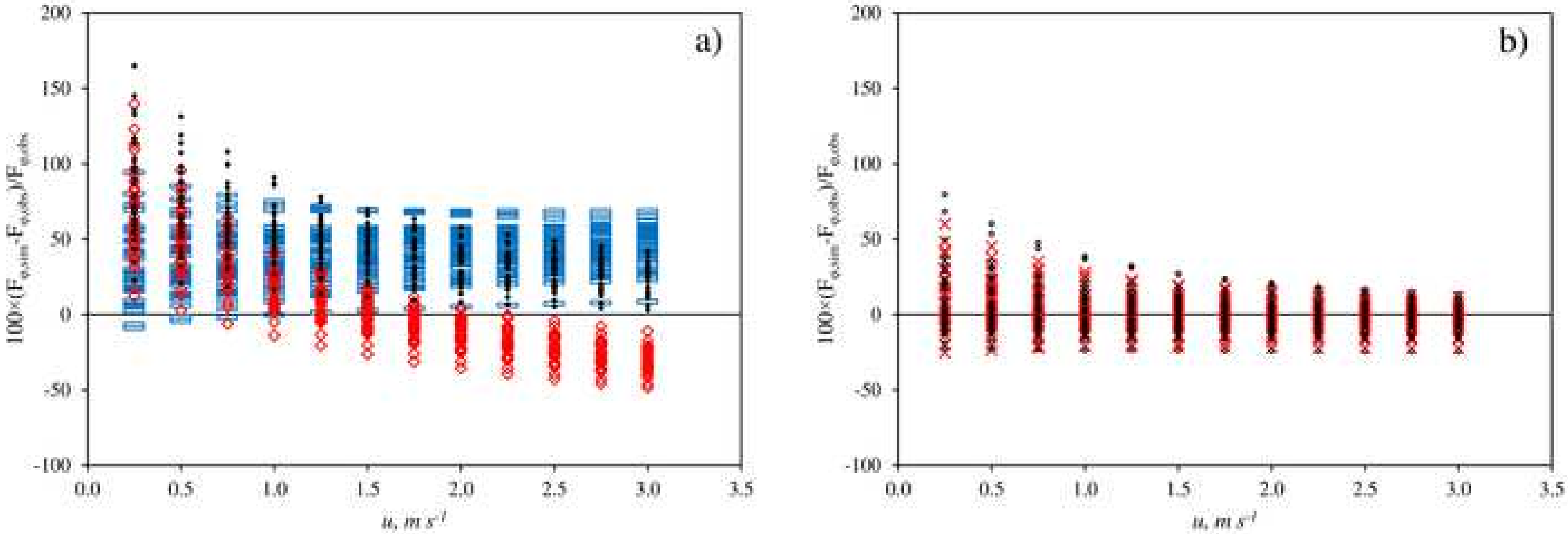

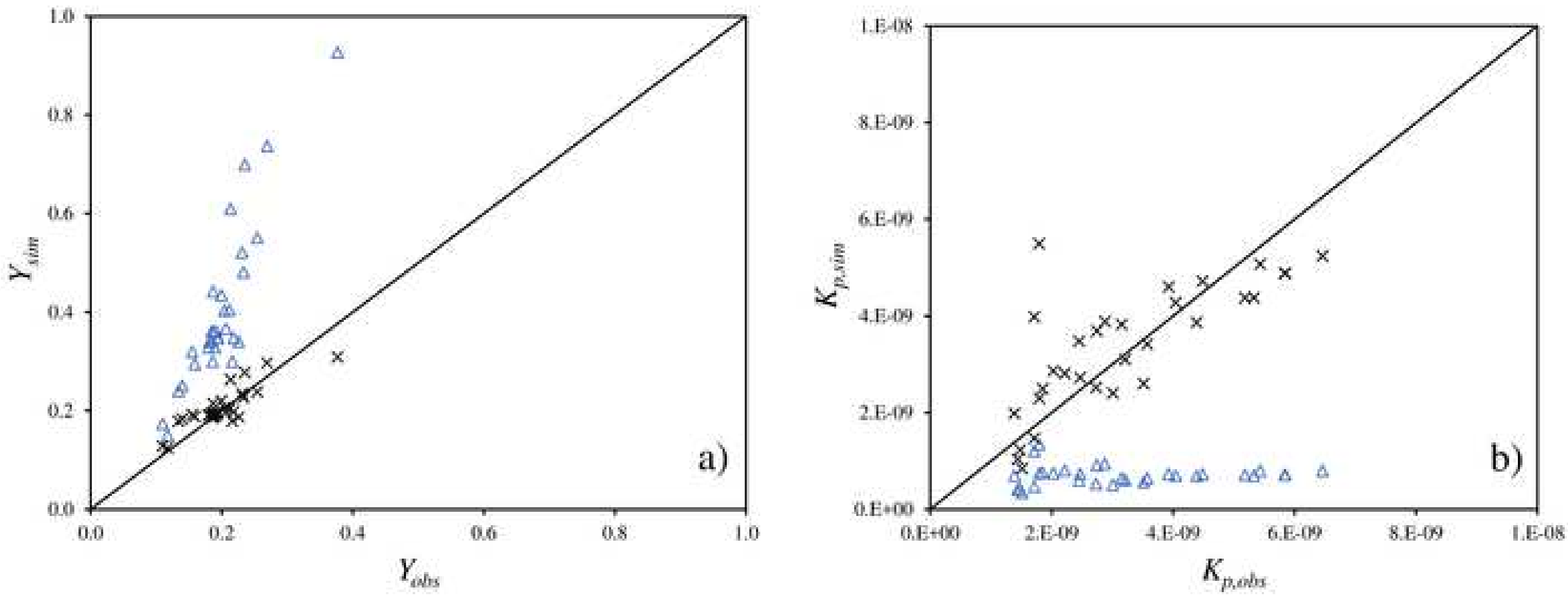

1.0
0.8
0.6
0.4
0.2
0.0
0.0
0.2
0.4
0.6
0.8
1.0
Y_{sim}
Y_{obs}
a)
1.E-08
8.E-09
6.E-09
4.E-09
2.E-09
0.E+00
0.E+00
2.E-09
4.E-09
6.E-09
8.E-09
1.E-08
$K_{p,sim}$
$K_{p,obs}$
b)

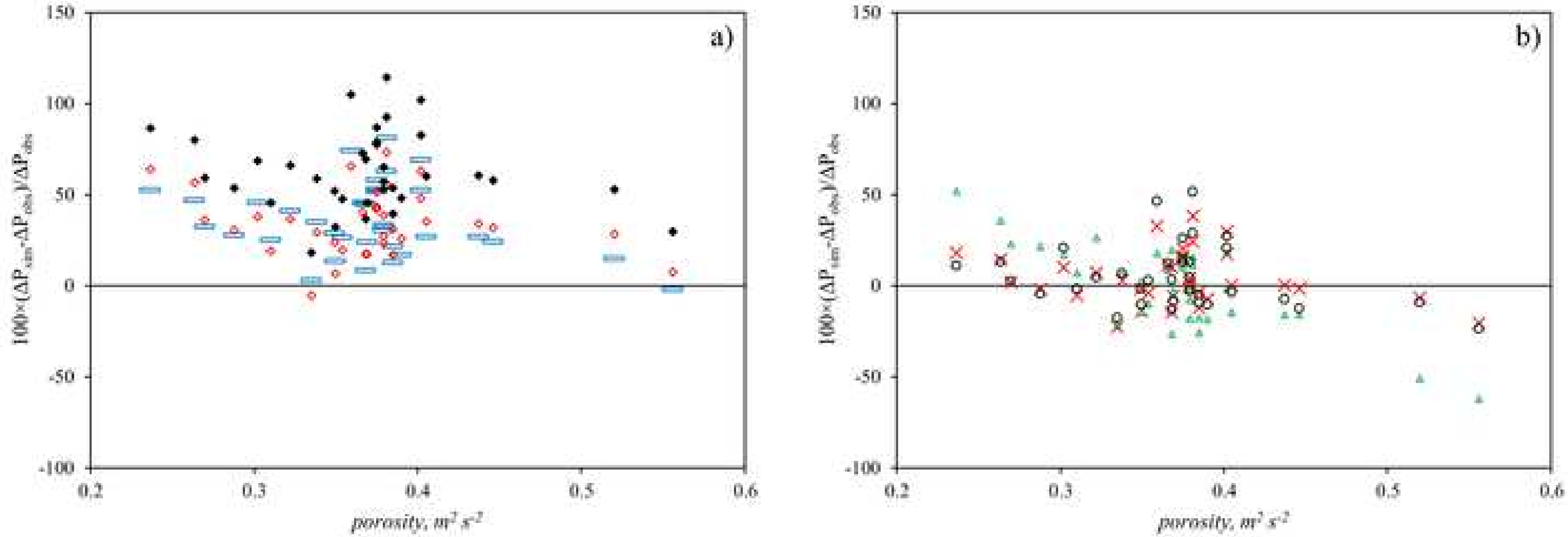

a)
b)
150
100
50
0
-50
-100
0.2
0.3
0.4
0.5
0.6
100×(ΔP_sim-ΔP_obs)/ΔP_obs
porosity, m² s⁻²

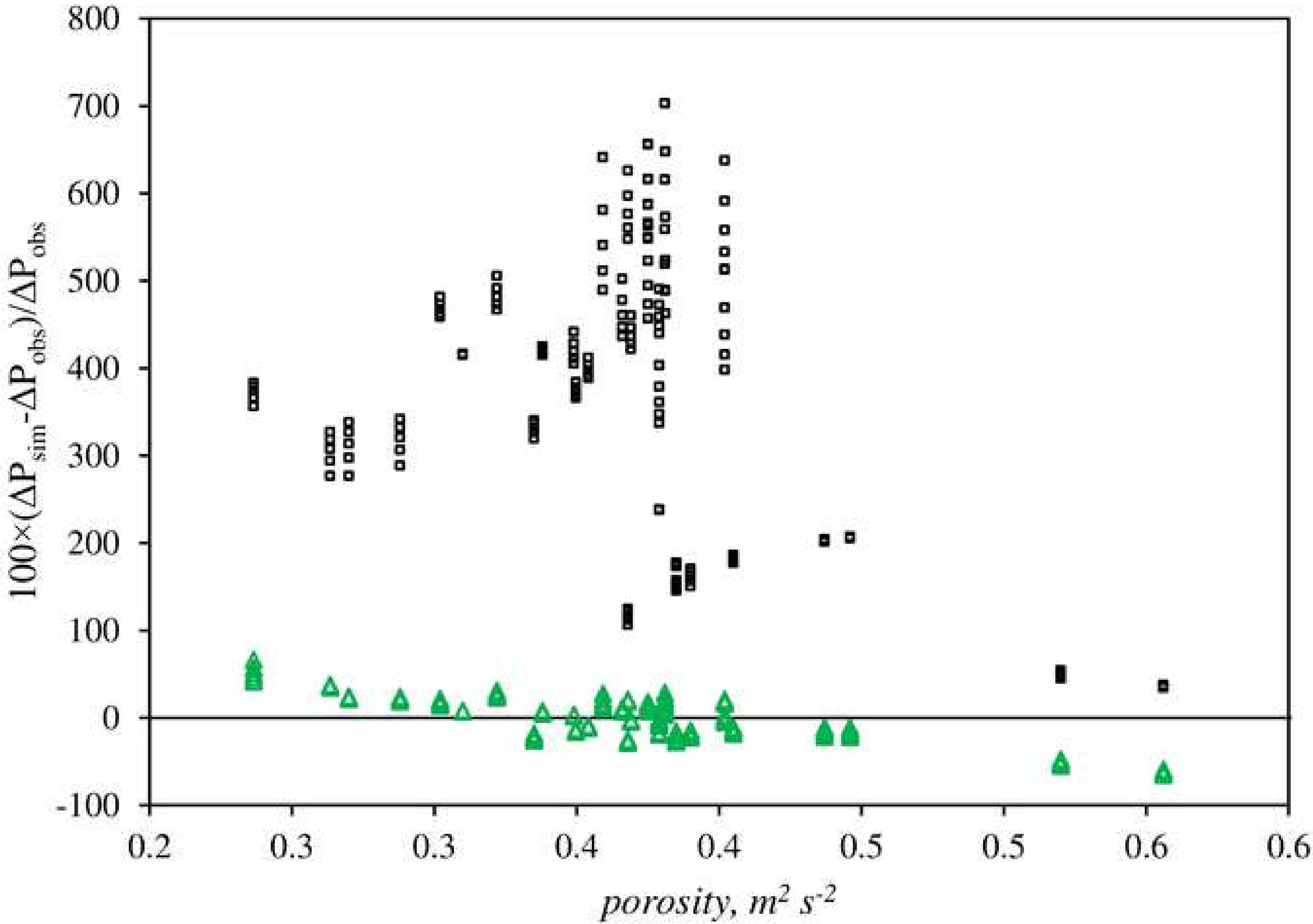
800
700
600
500
400
300
200
100
0
-100
0.2
0.3
0.3
0.4
0.4
0.5
0.5
0.6
0.6
100×(ΔPsim-ΔPobs)/ΔPobs
porosity, m2 s-2

Declaration of interests

☒ The authors declare that they have no known competing financial interests or personal relationships that could have appeared to influence the work reported in this paper.

☐The authors declare the following financial interests/personal relationships which may be considered as potential competing interests:

LOPEZ MARTINEZ ALEJANDRO - 45580435R

Digitally signed by LOPEZ MARTINEZ ALEJANDRO - 45580435R
DN: c=ES, serialNumber=IDCES-45580435R, givenName=ALEJANDRO, sn=LOPEZ MARTINEZ, cn=LOPEZ MARTINEZ ALEJANDRO - 45580435R
Date: 2020.01.17 14:04:33 +01'00'

Declaration of interests

☒ The authors declare that they have no known competing financial interests or personal relationships that could have appeared to influence the work reported in this paper.

☐The authors declare the following financial interests/personal relationships which may be considered as potential competing interests:

Signed: Francisco Domingo MOLINA AIZ

Declaration of interests

☑ The authors declare that they have no known competing financial interests or personal relationships that could have appeared to influence the work reported in this paper.

☐ The authors declare the following financial interests/personal relationships which may be considered as potential competing interests:

December 4th, 2019

Karlos Espinoza

Declaration of interests

☒ The authors declare that they have no known competing financial interests or personal relationships that could have appeared to influence the work reported in this paper.

☐The authors declare the following financial interests/personal relationships which may be considered as potential competing interests:

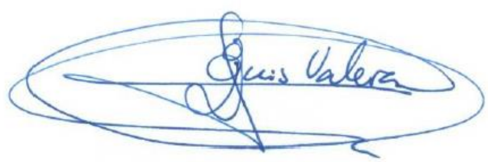

Fdo. Diego Luis Valera Martínez